Distributed optimization of the stochastic load of residential heat pumps for demand response

Uytterhoeven, Anke; Van Rompaey, Robbe; Helsen, Lieve; Bruninx, Kenneth

DOI
10.1016/j.enbuild.2025.115780

Publication date
2025

Document Version
Final published version

Published in
Energy and Buildings

Citation (APA)
Uytterhoeven, A., Van Rompaey, R., Helsen, L., & Bruninx, K. (2025). Distributed optimization of the stochastic load of residential heat pumps for demand response. *Energy and Buildings*, *342*, Article 115780. https://doi.org/10.1016/j.enbuild.2025.115780

Energy & Buildings 342 (2025) 115780

Contents lists available at ScienceDirect

Energy & Buildings

journal homepage: www.elsevier.com/locate/enbuild

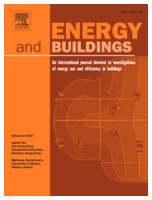

Distributed optimization of the stochastic load of residential heat pumps for demand response

Anke Uytterhoeven [a,b], Robbe Van Rompaey [c], Lieve Helsen [a,b], Kenneth Bruninx [a,d,*]

[a] KU Leuven, Department of Mechanical Engineering, Division of Applied Mechanics and Energy Conversion, Celestijnenlaan 300 box 2421, 3001, Leuven, Belgium
[b] EnergyVille, Thor Park 8310, 3600, Genk, Belgium
[c] KU Leuven, Department of Electrical Engineering, STADIUS, Kasteelpark Arenberg 10 box 2446, 3001, Leuven, Belgium
[d] TU Delft, Faculty of Technology, Policy and Management, Jaffalaan 5, 2628 BX, Delft, the Netherlands

ARTICLE INFO

Keywords:
Demand response
Distributed optimization
Stochastic model predictive control
Chance constraints
Affine disturbance feedback
Thermostatically controlled loads

ABSTRACT

The main aim of this paper is to illustrate the added value at system level of explicitly accounting for the closed-loop feedback aspect in the open-loop optimal control problem of model predictive control strategies for thermostatically controlled loads participating in demand response programs, when subject to uncertainties. To this end, an integrated system-level optimization problem is set up, merging an economic dispatch problem to represent the supply side and an open-loop stochastic optimal control problem incorporating affine disturbance feedback to represent the demand side. The incorporation of affine disturbance feedback enables the simultaneous optimal scheduling of the demand for electrical energy, reserve capacity and real-time flexibility required to guarantee thermal comfort at the demand side, thereby disclosing very valuable information for an aggregator or system operator, since the load uncertainty can be revealed and controlled ahead of real time. To solve the mathematically complex integrated problem, a distributed solution strategy based on the alternating direction method of multipliers is developed. With the help of an illustrative case study, it is demonstrated that the day-ahead coordination of the demand for reserve capacity in addition to the energy demand is able to reduce the system operating cost while guaranteeing thermal comfort, and hence, enables a more cost-efficient electrification of the residential heating sector. Cost reductions up to 10.7 % are shown to be achievable for a demand side consisting of 900 000 flexible heat pumps combined with low-temperature radiators.

1. Introduction

Decarbonizing the building heating sector requires adopting electricity-based heating and integrating them in a cost-efficient way into an electric power system dominated by variable renewables (RES) [1–3]. In this setting, thermostatically controlled loads (TCLs), such as heat pumps (HPs), play an important role, because of the high cumulated energy use, and the inherent flexibility offered by the thermal storage capacity of the building thermal mass and active energy storage devices if available [4–6]. The exploitation of this available flexibility can be established via demand response (DR) [7,8,35]. The main aim of DR is to let flexible end-consumers change their consumption pattern to better match the available supply, which is often achieved via price incentives [9]. Here, advanced control strategies play an important role, since residential consumers lack the required knowledge about how to optimally schedule the operation of their appliances and heating, ventilation and air-conditioning (HVAC) devices in response to changing price signals [10]. Besides, dynamic pricing without smart appliances, thus requiring manual interventions, is also shown to lead to user fatigue, resulting in very limited behavioral changes [11,36]. Hence, automated response technologies are recommended to facilitate the implementation of DR [9,12,36].

In this paper, we focus on DR involving model predictive control (MPC) applied to TCLs, with a particular focus on the consideration of uncertainties therein, at the building and system level. In doing so, we merge two streams in the scientific literature. A first stream focuses on the application of MPC at building level, in the context of optimal control of TCLs under uncertainty. Typically, these approaches (i) neglect the dynamic interaction between buildings as well as between buildings and the rest of the energy system, and (ii) assume all uncertainty on the heating demand must be managed locally by the MPC strategy. The second stream of literature pertains to energy system level studies accounting for the DR potential of TCLs in day-ahead scheduling or market clearing problems , i.e., on a national or supra-national electric power

* Corresponding author.
E-mail address: k.bruninx@tudelft.nl (K. Bruninx).

https://doi.org/10.1016/j.enbuild.2025.115780
Received 24 December 2024; Received in revised form 24 March 2025; Accepted 21 April 2025
Available online 25 April 2025

List of abbreviations

ADF	affine disturbance feedback
ADMM	alternating direction method of multipliers
DR	demand response
HVAC	heating, ventilation and air-conditioning
HP	heat pump
MPC	model predictive control
OCP	optimal control problem
OPF	optimal power flow
PV	photovoltaic
RES	renewable energy sources
RMPC	robust model predictive control
SMPC	stochatic model predictive control
SMPC^{ap}	stochastic model predictive control hedging against additive as well as parametric uncertainties
SOC	second order cone
TCL	thermostatically controlled load

List of symbols

Latin characters

$\dot{P}$	electric power [W]
$\dot{Q}$	thermal power [W]
$\mathbf{A}$	building model state space matrix A (states)
$\mathbf{B}$	building model state space matrix B (inputs)
$\mathbf{d}$	building model disturbances
$\mathbf{E}$	building model state space matrix E (disturbances)
$\mathbf{e}$	selection vector
$\mathbf{I}$	identity matrix
$\mathbf{p}$	latent variable aggregating all uncertainties
$\mathbf{q}$	auxiliary variable related to the second order cone constraints on the building model states [$°C^{1/2}$]
$\mathbf{r}$	auxiliary variable related to the second order cone constraints on the building model inputs [$W^{1/2}$]
$\mathbf{s}$	slack variable related to the building model state constraints [°C]
$\mathbf{T}$	transformation matrix
$\mathbf{u}$	building model inputs [W]
$\mathbf{x}$	building model states [°C]
$\mathbf{z}$	auxiliary optimization variables
B	total number of buildings constituting the demand side
c	cost [EUR]
cap	capacity of a generator [W]
COP	coefficient of performance
D	demand for electric energy [W h]
G	total number of (aggregated) generators constituting the supply side
K	prediction horizon
k	time (in discrete time domain)
n	number/amount
R	demand for reserve capacity [W]
res	residual of the iterative ADMM procedure
S	supply of electric energy [W h]
T	temperature [°C]
t	time (in continuous time domain)
V	supply of reserve capacity [W]
w	system-level uncertainty [W]
X	set of constraints restraining χ

Greek characters

α	participation factor defining the affine control scheme of a generator
ϵ	risk level
λ	dual variable of a constraint
ρ	ADMM penalty factor
Σ	variance
σ	standard deviation
χ	optimization strategy aggregating all optimization variables, including those directly involved in the coupling constraints

Special characters

$\mathbb{N}$	the set of integer numbers
$\mathfrak{o}$	optimization strategy aggregating all optimization variables, except for those directly involved in the coupling constraints
$\mathbb{R}$	the set of real numbers

Subscripts

0	initial value
amb	ambient
b	building index
$dual$	dual (feasibility)
g	generator index
gen	generation
hp	heat pump
i	building model state index
ia	indoor air
k	time index
$prim$	primal (feasibility)
rad	Radiator
s	building sample index
sol	solar (irradiance)
sup	supply
sys	system level
$trad$	traditional

Superscripts

EN	energy
l	ADMM iteration index
max	Maximum value
min	minimum value
r	root form
RE	reserve capacity
REa	reserve capacity activation
REp	reserve capacity provision
sh	space heating
T	transpose

Operators

$\tilde{\cdot}$	uncertain variable
$\bar{\cdot}$	mean value
$\Delta(.)$	Uuncertainty band around the mean value of a stochastic variable
$\mathbb{E}[.]$	expected value
$(\|\|\|.\|\|\|)$	norm
$P(.)$	probability

system scale. These studies typically focus on the demand for energy, not the demand for real-time flexibility, nor the interaction between these two commodities for TCLs with MPC.

1.1. Model predictive control on building level

In the first stream of literature, discussed below, authors assess the day-ahead DR scheduling problem under uncertainty via a bottom-up approach, from the consumer perspective. These approaches typically implement an MPC strategy that is reacting to an external price signal expressing the DR request. The MPC problem is formulated as a stochastic/robust optimal control problem (OCP) in order to guarantee thermal comfort, as well as to guarantee the feasibility of the scheduled load profile in real time, despite possible uncertainty manifestations. For example, Garifi et al. [38] proposed a chance constrained MPC algorithm, which optimally schedules the operation of the combination of an HVAC system, uncontrollable loads, a local PV installation and a battery system in a residential building, in response to a grid load reduction request, at minimal operating cost. Two sets of chance constraints were implemented, to guarantee the satisfaction of the load reduction, as well as of the thermal comfort, with high probability. The considered uncertainties include the available PV power and the outdoor air temperature, which are assumed to be normally distributed (and possibly time-dependent). Wang et al. [39] considered a robust optimization method for day-ahead household load scheduling in response to a time-varying electricity price profile. Different levels of conservatism were allowed, enabling a trade-off between cost and thermal comfort. The loads considered in the scheduling problem include controllable loads affected by uncertainty (i.e., an air conditioning unit and an electric water heater), uncontrollable loads, uninterruptible loads, interruptible loads, and an (electric) energy storage device. The control strategy explicitly accounts for uncertainties on the outdoor temperature and the hot water demand, which were modeled with the help of uncertainty sets surrounding the forecast values. Langer et al. [13] compare robust and chance-constrained MPC approaches to hedge heating schedules against building model estimation errors. They illustrate that chance-constrained MPC outperforms the robust approach. Parastoo et al. [14] focus on model and forecast uncertainty in chance-constrained MPC. They illustrate that this leads to better thermal comfort while limitedly increasing energy use in a case study of a single building.

The consumer-oriented approaches discussed above neglect, or even deliberately prohibit the closed-loop corrective behavior of MPC, and thus, do not incorporate affine disturbance feedback (ADF). As such, they opt for very conservative control strategies, where the impact of uncertainties is fully managed at consumer level. To address this conservatism, researchers have developed robust/stochastic MPC (RMPC/SMPC) approaches considering ADF. Here, the idea is to parametrize the control inputs as affine functions of the preceding uncertainties, in order to mimic the closed-loop corrective behavior of MPC in the open-loop control problem. As such, not only the demand for electrical energy, but also the demand for real-time flexibility is made explicit. As we will illustrate in the following paragraphs, up to now, this feature has been merely considered in the context of building climate control, but has not yet been exploited for demand response purposes on the system level (Section 1.2).

Maasoumy et al. [15] considered imperfect predictions of the ambient air temperature, solar radiation, and internal heat gains from occupants and equipment, and coped with this uncertainty by adopting an RMPC strategy with ADF. In [16], Oldewurtel et al. applied analytically reformulated chance constraints, combined with ADF, to cope with assumed Gaussian uncertainty on the outside air temperature, the wet-bulb temperature and the incoming solar radiation. The SMPC strategy was shown to outperform both conventional rule-based control and deterministic MPC, by achieving a better trade-off between energy use and probability of thermal comfort violations. In related work [16–18], a tractable approximation of chance constrained SMPC combined with ADF was developed and applied, in order to cope with uncertainty on the weather and occupant behavior.

More recently, the focus has shifted towards the uncertainty on building model parameters. Nagpal et al. [19] considered a dedicated RMPC strategy with feedback applied to both a residential and an office building. Variations of a selection of the parameters of a one-zone four-states building model, being the heat transfer coefficient between the zone air and internal mass and the heat transfer coefficient between the zone air and ambient temperature, were included in an RMPC formulation as polytopic uncertainties, characterized by a minimum and maximum value. Bunnig et al. [20] combine RMPC with affine policies using data-driven demand forecasting, avoiding physics-based building models. Their work shows how heat pumps can offer more frequency regulation reserves while maintaining user comfort by integrating affine policies. To tackle the combination of uncertainties on the disturbance forecasts (i.e., weather and occupant behavior) and on the building model parameters, Uytterhoeven et al. [21] recently developed an stochastic chance-constrained MPC strategy for building climate control incorporating ADF.

1.2. Demand response potential of TLCs on power system level

Also for DR studies focusing on the system level – the second stream of literature this paper connects to – there has been an increasing interest to explicitly consider uncertainties in the decision-making process, in order to guarantee the feasibility and optimality of the determined load schedules in real time [22–24,39]. Although there is a vast amount of research available targeting uncertainty in real-time control (see e.g., [24–26]), the uncertainty is especially important in day-ahead planning problems, since they require forecasts over a longer timescale, which are inevitably more uncertain [27]. Here, the flexible load model is part of a larger energy system optimization problem or equilibrium model, using OCP formulations to describe the TCL behavior (similar to MPC). These approaches acknowledge that the demand can be uncertain, and explicitly optimize the actions required to cope with this load uncertainty. The load uncertainty is typically assumed to be known and uncontrollable.

Vrakopoulou et al. [28,29] developed a multi-period chance constrained optimal power flow (OPF) formulation that co-optimizes energy and reserves provided by both generators and controllable TCLs for the upcoming day to guarantee minimal operating cost, while taking into account uncertainty on the forecasts of the renewable power generation and the TCL behavior via scenarios. A similar problem setting was considered by Zhang et al. [30], who solved a single-period (instead of a multi-period) chance constrained OPF via distributionally robust optimization. Good et al. [31] assessed the DR problem rather from a market oriented perspective. They looked at aggregated TCLs whose market participation was modeled with the help of a two-stage stochastic problem, with the aim to minimize the overall expected day-ahead energy costs, as well as imbalance costs for deviations from the day-ahead position as a consequence of demand forecast uncertainty. Another two-stage stochastic problem can be found in the work of Kou et al. [32], who considered a distribution system operator that coordinates the use of the flexibility of a large number of residential TCLs (via an aggregator) to maximize social welfare, while explicitly mitigating the impact of a wide range of uncertainties on the DR performance. Also Bruninx et al. [64,65] explicitly accounted for load uncertainties in a demand response context. In [64], the authors solved a multi-period deterministic unit commitment model to determine the optimal day-ahead power plant schedule, with probabilistic power balancing and reserve constraints to cope with uncertainties. The considered uncertainties include the stochastic renewable electricity generation, and the limited controllability of the residential electric heating systems providing load shifting and ancillary services. In [65], Bruninx et al. assessed a similar scheduling problem, although this time without reserve provision by the TCLs, from a market perspective, by studying the strategic interactions between an aggregator, its consumers, and the day-ahead market,

with the help of a bi-level optimization framework. Chance constraints were used to cope with the uncertainty, forcing the aggregator to procure sufficient electricity in the day-ahead market to be able to cover the demand of its consumers in accordance with the imposed level of risk aversion.

A few authors have attempted, like we do in this paper, to connect state-of-the-art MPC strategies accounting for uncertainty with system-level day-ahead scheduling models to study the DR with TCLs. Closest to our approach is the work of Diekerhof et al. [40] and Lakeshwara and Sharma [41]. Diekerhof et al. [40] considered an RMPC strategy as part of a larger hierarchical DR framework, used for the day-ahead scheduling of flexible heat pumps (by implementing the alternating direction method of multipliers (ADMM) for distributed optimization). In the proposed framework, an aggregator coordinates the heat pump demand via an exchange of price vectors, in order to pursuit a system-level objective, being either a minimization of the energy procurement cost, or peak shaving. The TCLs, on the other hand, respond to the coordination signals received from the aggregator, while potentially optimizing an additional local objective. The heat pump operation is optimized in a robust way, hedging against uncertainty on the thermal demand of the building, in order to avoid real-time power adjustments to the pre-calculated operational schedule and as such ensure compliance with the DR request. In Lakeshwara and Sharma [41] show how hierarchical DR control can be implemented via Lagrangian relaxation. Leveraging RMPC for each TCL, they track a load set-point in real time while managing the uncertainties of the building models and outside temperature. Feedback is, however, not considered, resulting in conservative control policies.

1.3. Research gap and contributions

In summary, while the superior performance of SMPC with disturbance feedback has been illustrated in consumer-centered work (Section 1.1), state-of-the-art system-level DR studies are limited to RMPC without ADF (Section 1.2). This implies that real-time adjustments to the scheduled control strategy of TCLs are prohibited, thereby fully managing the uncertainty on consumer level. The system-level oriented literature illustrates that load uncertainty can be effectively managed at system level as well.

This paper fills this research gap by explicitly accounting for the closed-loop feedback aspect in the open-loop OCP of MPC strategies via ADF for TCLs participating in DR programs. This enables optimal coordination of the energy demand and uncertainty. This approach discloses very valuable information for an aggregator or system operator, since it not only allows to characterize the load uncertainty in detail, but moreover allows to optimize it ahead of real time. As such, this stochastic MPC incorporating ADF enables the orchestration of an optimal balance between the supply of and demand for energy as well as balancing services, yielding system-wide benefits. Furthermore, a trade-off between the degree of uncertainty management at building versus at system level is enabled, which may facilitate a more cost-effective use of the demand side flexibility offered by TCLs. This may establish a reduction of the overall system operating cost, and may guarantee a more cost-efficient electrification of the residential space heating sector.

1.4. Outline

The remainder of this paper is organized as follows. Section 2 discusses the considered energy system optimization problem, incorporating an open-loop stochastic OCP with ADF to represent the demand side and an economic dispatch problem to represent the supply side, as well as the solution strategy for this integrated problem. Section 3 presents the data and assumptions in our case study, investigating the impact of the coordination of the demand for real-time flexibility in addition to the demand for energy on the overall system operating cost. The results of this case study are discussed in Section 4, after which Section 5 concludes.

2. Methodology

As the interaction between the demand side and the supply side is of paramount importance when investigating the effects of DR [35,36], an integrated system-level optimization problem needs to be developed to properly determine the overall system operating cost. This problem formulation is set up in Section 2.1, considering the constraints associated with the demand side, consisting of residential buildings equipped with heat pumps, each assumed to be managed by an SMPC^{ap} (stochastic model predictive control hedging against **a**dditive as well as **p**arametric uncertainties via affine disturbance feedback) strategy (Section 2.1.1), and the supply side, consisting of electricity generation units (Section 2.1.2). In both cases, we hedge the schedules against uncertainty via chance constrained programming.[1] Assuming an affine disturbance feedback at the demand side and an affine control policy at the supply side facilitates recasting the resulting formulations as convex optimization problems, which can be merged in a convex integrated system-level optimization problem. Subsequently, in Section 2.2, a distributed solution approach based on ADMM is proposed to solve this mathematically complex problem.

The considered open-loop stochastic OCP formulation[2] to represent the demand side builds upon our previous work [21], focusing on the development of an SMPC^{ap} strategy for building climate control under combined additive and parametric uncertainties. Thanks to the incorporation of ADF in the open-loop control problem, it allows optimizing the demand for electrical energy as well as the demand for real-time flexibility. The proposed integrated system-level optimization problem aims to exploit this additional degree of freedom for the benefit of the central energy system when coordinating the demand of a group of TCLs. In Section 4, the resulting overall system operating cost will be compared to that of an equivalent case without ADF, where the coordination of the demand for reserve capacity and real-time flexibility is disabled. As discussed above, such a strategy without ADF can be considered as the current state-of-the-art for DR with MPC under uncertainty [38–40], albeit our approach additionally considers parametric uncertainties.

2.1. Integrated system-level optimization problem

The integrated system-level optimization problem (1) merges an economic dispatch problem, representing the supply side, and a set of open-loop stochastic OCPs[2], one for each considered building, representing the demand side. This problem mimics the day-to-day operation of the power system, and schedules available electricity generation assets to meet the demand at minimum total expected operating cost.

$$\min_{\substack{\{\chi_b\}_{b=1\dots B}\\ \{\chi_g\}_{g=1\dots G}}} \sum_{g=1}^{G} c_g^{EN} + c_g^{REp} + c_g^{REa} \tag{1a}$$

subject to

[1] Chance constrained programming allows enforcing constraints in an optimization problem with a predefined probability. For more information, see Nemirovski and Shapiro [37].

[2] Since the focus is on the day-ahead scheduling, only the open-loop OCP of the MPC strategy is considered. The subsequent solution of the closed-loop OCP throughout the day is not further considered. The absence of a receding horizon approach with closed-loop disruptions is why the considered implementation is referred to as an OCP, rather than as an MPC strategy in the strict sense.

$$\begin{cases} \text{Demand side constraints:} \\ \quad \left(\bar{\mathbf{D}}_b, \mathbf{R}_b, \mathbb{o}_b\right) = \chi_b \in X_b \qquad \forall b \\ \text{Supply side constraints:} \\ \quad \left(\bar{\mathbf{S}}_g, \mathbf{V}_g, \mathbb{o}_g\right) = \chi_g \in X_g \qquad \forall g \\ \text{Coupling constraints:} \\ \quad \{\bar{\mathbf{S}}_g\}_{g=1\dots G} \leftrightarrow \{\bar{\mathbf{D}}_b\}_{b=1\dots B}, \bar{\mathbf{D}}_{trad} \\ \quad \{\mathbf{V}_g\}_{g=1\dots G} \leftrightarrow \{\mathbf{R}_b\}_{b=1\dots B}, \sigma_{sys} \end{cases} \tag{1b}$$

The total expected operating cost of the electric power supply system in the day-ahead stage entails of the costs of energy, c_g^{EN}, reserve capacity provision, c_g^{REp}, and reserve capacity activation (i.e., balancing energy), c_g^{REa}. These costs are determined by the stochastic supply scheduled for each generator g, $\tilde{\mathbf{S}}_g = \{\bar{S}_{g,k} + \delta S_{g,k}\}_{k=0\dots K}$, which is split up in a supply of energy, $\bar{\mathbf{S}}_g$, and a supply of reserve capacity, $\mathbf{V}_g$ (related to $\Sigma_{\mathbf{S}_g}$), where the latter is a common way to cope with load uncertainty (and thus, to accommodate demand for real-time flexibility). The same distinction is made for the stochastic, flexible demand of each building b accommodating flexible heat pumps for space heating, $\tilde{\mathbf{D}}_b = \{\bar{D}_{b,k} + \delta D_{b,k}\}_{k=0\dots K}$, resulting in a demand for energy $\bar{\mathbf{D}}_b$, and a demand for reserve capacity, $\mathbf{R}_b$ (related to $\Sigma_{\mathbf{D}_b}$). The supply of energy, $\{\bar{\mathbf{S}}_g\}_{g=1\dots G}$, covers the flexible demand for energy from the heat pumps, $\{\bar{\mathbf{D}}_b\}_{b=1\dots B}$, as well as the inflexible electricity demand, $\bar{\mathbf{D}}_{trad}$, encompassing all residual electricity demand (i.e., the remaining demand after the subtraction of the available renewable generation). The supply of reserve capacity, $\{\mathbf{V}_g\}_{g=1\dots G}$, covers the demand for reserve capacity of the flexible heat pumps, $\{\mathbf{R}_b\}_{b=1\dots B}$, as well as the system-level uncertainty, $\tilde{\mathbf{w}}_{sys} = \{\delta w_{sys,k}\}_{k=0\dots K}$. This system-level uncertainty represents the uncertainty on the traditional demand, the uncertainty on the renewable power generation, as well as the uncertainty related to the conventional generation, such as unplanned outages, etc. It is assumed to be Gaussian, with a zero mean, and variance $\Sigma_{sys,k}$.

Note that the operational decisions, or said differently, the strategy χ of each building (subscript b) and each generator (subscript g) do not only determine the demand for/supply of energy and reserve capacity, but also some other operational decisions that are not directly involved in the coupling constraints. These are represented by $\mathbb{o}$. Furthermore, each strategy χ belongs to a set of strategies X, which is defined by a number of equality and inequality constraints, constituting the sub-problems of each building or generator.

In the following sections, each of these sub-problems is further elaborated on, thereby defining the demand side constraints in Section 2.1.1, the supply side constraints in Section 2.1.2, the coupling constraints in Section 2.1.3, and the objective function in Section 2.1.4. The resulting formulation of the integrated optimization problem is summarized in Section 2.1.5.

2.1.1. Demand side constraints

Each building is assumed to be equipped with a heat pump for space heating and to be controlled by an SMPC^{ap} strategy. As such, the set of feasible strategies X_b for a particular building b can be defined in its most general form by the following set of constraints.

$$\tilde{\mathbf{x}}_{b,k+1} = \tilde{\mathbf{A}}_b \tilde{\mathbf{x}}_{b,k} + \tilde{\mathbf{B}}_b \tilde{\mathbf{u}}_{b,k} + \tilde{\mathbf{E}}_b \tilde{\mathbf{d}}_{b,k} \quad \forall k \tag{2a}$$

$$P(\tilde{\mathbf{x}}_{b,k} + \mathbf{s}_{b,k} \geq \mathbf{x}_{b,k}^{min}) \geq 1 - \boldsymbol{\epsilon}_{\mathbf{x}_{b,k}} \quad \forall k \tag{2b}$$

$$P(\tilde{\mathbf{x}}_{b,k} - \mathbf{s}_{b,k} \leq \mathbf{x}_{b,k}^{max}) \geq 1 - \boldsymbol{\epsilon}_{\mathbf{x}_{b,k}} \quad \forall k \tag{2c}$$

$$\mathbf{s}_{b,k} \geq \mathbf{0}_{n_x} \quad \forall k \tag{2d}$$

$$P(\tilde{\mathbf{u}}_{b,k} + \mathbf{r}_{b,k} \geq \mathbf{0}_{n_u}) \geq 1 - \boldsymbol{\epsilon}_{\mathbf{u}_{b,k}} \quad \forall k \tag{2e}$$

$$P(\tilde{\mathbf{u}}_{b,k} - \mathbf{r}_{b,k} \leq \mathbf{u}_{b,k}^{max}) \geq 1 - \boldsymbol{\epsilon}_{\mathbf{u}_{b,k}} \quad \forall k \tag{2f}$$

$$\mathbf{r}_{b,k} \geq \mathbf{0}_{n_u} \quad \forall k \tag{2g}$$

$$\mathbf{x}_b(0) = \mathbf{x}_{b,0} \tag{2h}$$

$$\mathbf{u}_b(0) = \mathbf{u}_{b,0} \tag{2i}$$

Here, $\{\tilde{\mathbf{x}}_{b,k} \in \mathbb{R}^{n_x}\}_{k=0\dots K+1}$ represents all stochastic system states over the prediction horizon K, being the indoor air temperature as well as all relevant temperatures of the building construction elements and of the heating system (which can be easily extended to the complete HVAC system). $\{\mathbf{s}_{b,k} \in \mathbb{R}^{n_x}\}_{k=0\dots K+1}$ represents the slack variables relaxing the state constraints. $\{\tilde{\mathbf{u}}_{b,k} \in \mathbb{R}^{n_u}\}_{k=0\dots K}$ in turn represents the stochastic[3] thermal power inputs delivered by the heat supply system during one time step Δt. Finally, $\{\tilde{\mathbf{d}}_{b,k} \in \mathbb{R}^{n_d}\}_{k=0\dots K}$ represents the uncertain point forecasts of the disturbances affecting the system, such as weather and occupant behavior.

The state space Eq. (2a) describes the dynamics of the building envelope and heating system with the help of the stochastic state space matrices $\tilde{\mathbf{A}}_b \in \mathbb{R}^{n_x \times n_x}$, $\tilde{\mathbf{B}}_b \in \mathbb{R}^{n_x \times n_u}$ and $\tilde{\mathbf{E}}_b \in \mathbb{R}^{n_x \times n_d}$, constituting the uncertain building controller model. This constraint determines the evolution of the system states $\tilde{\mathbf{x}}_{b,k+1}$ as a function of the preceding states $\tilde{\mathbf{x}}_{b,k}$, heat inputs $\tilde{\mathbf{u}}_{b,k}$ and disturbances $\tilde{\mathbf{d}}_{b,k}$. The states are constrained by a lower and upper bound, $\{\mathbf{x}_{b,k}^{\min}\}_{k=0\dots K+1}$ and $\{\mathbf{x}_{b,k}^{\max}\}_{k=0\dots K+1}$, in Eqs. (2b) and (2c). Because of the stochasticity of the states, these constraints need to be imposed as chance constraints with risk level $\{\boldsymbol{\epsilon}_{\mathbf{x}_{b,k}}\}_{k=0\dots K+1}$, rather than as hard constraints. When applied to the indoor temperature, these state constraints (approximately[4]) denote the thermal comfort requirements. These requirements cannot always be satisfied, e.g., after a perturbation due to an uncertainty manifestation. To prevent the model from becoming infeasible in these cases, the state constraints are relaxed with the help of the slack variables $\mathbf{s}_{b,k}$ that are penalized in the pursued objective function at a very high value.[5] The inputs are in turn limited by a lower and upper power bound in Eqs. (2e) and (2f), reflecting the technical limits of the heating system. Again, these constraints need to be reformulated as chance constraints, and can be relaxed with the help of the slack variables $\mathbf{r}_{b,k}$ to avoid infeasibility. Finally, the current conditions, represented by $\mathbf{x}_{b,0}$ and $\mathbf{u}_{b,0}$, are taken into account as initial values for the states and inputs in Eqs. (2h) and (2i).

The general formulation of Problem (2) can be reformulated into a proper convex stochastic formulation (Problem (3)), by applying the following manipulations: i) the elaboration of the mean $\bar{\cdot}$ and covariance matrices $\Sigma_{\cdot}$ of all stochastic variables, ii) the introduction of the latent variable $\tilde{\mathbf{p}}_b$, aggregating all additive and parametric uncertainties in one single vector, from which the relevant uncertainties can be extracted with the help of appropriate selection matrices $\mathbf{T}_{\cdot}$, iii) the switch to a root form notation for the covariance matrices (with $\Sigma_{\cdot} = \Sigma_{\cdot}^{r}\,\Sigma_{\cdot}^{rT}$), iv) the introduction and reformulation of chance constraints into second order cone (SOC) constraints, and v) the implementation of ADF by reformulating the control inputs as an affine function of the preceding perturbations with the help of the feedback gain matrix $\mathbf{T}_{\mathbf{u}_b}$ (see Eq. (3j)), serving as an additional optimization variable. Note that the inclusion of ADF makes it possible to mimic and optimize the closed-loop behavior of the MPC in the open-loop OCP. Hence, it is a key aspect of the proposed methodology, allowing for a characterization and optimization of the load uncertainty ahead of real time. In addition to the above mentioned manipulations, the following assumptions are required to end up with a convex stochastic problem formulation: i) the original deterministic OCP formulation is convex, ii) the products of stochastic variables are neglected, and, iii) the chance constraints are reformulated for every distinct state and input based on its marginal distribution, which

[3] The stochasticity of the control inputs is caused by the implementation of ADF, formulating the control inputs as an affine function of the preceding uncertainty manifestations, which are not known beforehand.

[4] In reality, thermal comfort is determined by a wide variety of factors, such as metabolic factors, humidity level, human body thermal radiation, etc. [42]. However, including detailed comfort models in the OCP could lead to a computationally intractable problem [43,44].

[5] In order not to detract from the main message, this additional component, consisting of the sum of all slack variables over the optimization horizon, multiplied by a large factor (here, 10^6), is not explicitly mentioned in the objective functions throughout this paper.

is assumed to be normal. For more details, the interested reader is referred to our previous work [21], thoroughly discussing the derivation of the SMPC^{ap} problem formulation, and the inclusion of ADF therein. The convex stochastic formulation of Problem (3) builds on the SMPC^{ap} problem formulation derived in Uytterhoeven et al. [21], with the following additional simplifications and additions: (i) a heat supply system model has been added, being a single heat pump with coefficient of performance (COP) $\{\overline{COP}^{sh}_{b,k}\}_{k=0\dots K}$,[6] electrical power input $\{\bar{P}^{sh}_{hp,b,k}\}_{k=0\dots K}$ and thermal power supply $\{\bar{Q}_{sup,b,k}\}_{k=0\dots K}$, (ii) the demand for space cooling and domestic hot water has been omitted, and (iii) no auxiliary resistance heater has been considered.

$$\bar{\mathbf{x}}_{b,k+1} = \bar{\mathbf{A}}_b\,\bar{\mathbf{x}}_{b,k} + \bar{\mathbf{B}}_b\,\bar{u}_{b,k} + \bar{\mathbf{E}}_b\,\bar{\mathbf{d}}_{b,k} \quad \forall k \tag{3a}$$

$$\begin{aligned}\Sigma^r_{\mathbf{x}_{b,k+1}} = {} & (\bar{\mathbf{x}}^T_{b,k} \otimes \mathbf{I}_{n_x})\Sigma^r_{\mathbf{A}_b} + \bar{\mathbf{A}}_b\,\Sigma^r_{\mathbf{x}_{b,k}} \\ & + \bar{u}_{b,k}\,\Sigma^r_{\mathbf{B}_b} + \bar{\mathbf{B}}_b\,\Sigma^r_{u_{b,k}} \\ & + (\bar{\mathbf{d}}^T_{b,k} \otimes \mathbf{I}_{n_x})\Sigma^r_{\mathbf{E}_b} + \bar{\mathbf{E}}_b\,\Sigma^r_{\mathbf{d}_{b,k}} \quad \forall k\end{aligned} \tag{3b}$$

$$\bar{x}_{b,i,k} + s_{b,i,k} \geq x^{min}_{b,i,k} + \Phi^{-1}(1-\epsilon_{x_{b,i,k}})\,q_{b,i,k} \quad \forall i,k \tag{3c}$$

$$\bar{x}_{b,i,k} - s_{b,i,k} \leq x^{max}_{b,i,k} - \Phi^{-1}(1-\epsilon_{x_{b,i,k}})\,q_{b,i,k} \quad \forall i,k \tag{3d}$$

$$q_{b,i,k} \geq \|\Sigma^r_{x_{b,i,k}}\|_2 \quad \forall i,k \tag{3e}$$

$$s_{b,i,k} \geq 0 \quad \forall i,k \tag{3f}$$

$$\bar{u}_{b,k} \geq 0 + \Phi^{-1}(1-\epsilon_{u_{b,k}})\,r_{b,k} \quad \forall k \tag{3g}$$

$$\bar{u}_{b,k} \leq u^{max}_{b,k} - \Phi^{-1}(1-\epsilon_{u_{b,k}})\,r_{b,k} \quad \forall k \tag{3h}$$

$$r_{b,k} \geq \|\Sigma^r_{u_{b,k}}\|_2 \quad \forall k \tag{3i}$$

$$\Sigma^r_{\mathbf{u}_b} = \mathbf{T}_{\mathbf{u}_b}\,\Sigma^r_{\mathbf{p}_b} \tag{3j}$$

$$\mathbf{x}_{\mathbf{b}}(0) = \mathbf{x}_{b,0} \tag{3k}$$

$$u_b(0) = u_{b,0} \tag{3l}$$

$$\bar{u}_{b,k} = \bar{Q}_{sup,b,k} = \overline{COP}^{sh}_{b,k}\,\bar{P}^{sh}_{hp,b,k} \quad \forall k \tag{3m}$$

$$u^{max}_{b,k} = \overline{COP}^{sh}_{b,k}\,\bar{P}^{sh,max}_{hp,b,k} \quad \forall k \tag{3n}$$

Note that the stochastic OCP formulation above incorporates ADF. The equivalent case without ADF can be seen as a special form of this problem formulation, which is obtained by forcing the selection matrix $\mathbf{T}_{\mathbf{u}_b}$ to be a zero matrix. The demand for electric energy $\bar{D}_{b,k}$ is equal to the heat pump electricity consumption during a time step Δt (Eq. (3o)). The demand for reserve capacity $R_{b,k}$, on the other hand, can be represented with the help of the auxiliary variable $r_{b,k}$, which is closely related to (i.e., bound from below by) the standard deviation of the stochastic demand $\tilde{D}_{b,k}$. Note that $r_{b,k}$ is chosen as a proxy for the standard deviation, instead of the root form $\Sigma^r_{D_{b,k}}$, since $r_{b,k}$ represents the uncertainty at a certain time step with the help of one single value, whereas in $\Sigma^r_{D_{b,k}}$, the uncertainty is distributed over multiple vector elements.

$$\bar{D}_{b,k} = \bar{P}^{sh}_{hp,b,k}\,\Delta t \quad \forall k \tag{3o}$$

$$R_{b,k} = \frac{r_{b,k}}{\overline{COP}^{sh}_{b,k}} \quad \forall k \tag{3p}$$

2.1.2. Supply side constraints

The considered supply side problem is a stylized version of an economic dispatch problem, stripped down to its essence, where ramping constraints, minimum on- and off-times, and start-up costs are neglected.[7]

In order to determine the supply of energy and reserve capacity of each (aggregated) generating unit g, we implement an affine control scheme, in analogy with ADF incorporated in the demand side constraints. By doing so, the generator output $\tilde{P}_{gen,g,k}$ can be written as a function of the uncertain demand (see Eqs. (3o) and (3p), thus exploiting the substantiated, bottom-up characterization established by the demand side constraints. Following Bienstock et al. [46], all conventional generators are assumed to modulate their output in response to real-time fluctuations in a proportional way with the help of the proportionality coefficients $\alpha_{g,k}$, as expressed by Eqs. (4a) and (4b), where these proportionality coefficients serve as additional optimization variables.

$$\tilde{\bar{P}}_{gen,g,k} = \bar{\tilde{P}}_{gen,g,k} + \alpha_{g,k}\left(\sum_{b=1}^{B}\frac{\delta D_{b,k}}{\Delta t} + \delta w_{sys,k}\right) \quad \forall g,k \tag{4a}$$

$$\alpha_{g,k} \geq 0 \quad \forall g,k \tag{4b}$$

The output of each generator becomes a function of the Gaussian random variables $\delta D_{b,k}$ and $\delta w_{sys,k}$. Because of its consequent stochasticity, the technical constraints regarding the output of a particular generator g, taking into account its minimal (0) and maximal (cap_g) capacity, can no longer be imposed as hard constraints, but instead need to be expressed as chance constraints with associated risk level $\epsilon_{\tilde{P}_{gen,g,k}}$.

$$P(\tilde{\bar{P}}_{gen,g,k} \geq 0) \geq 1 - \epsilon_{\tilde{P}_{gen,g,k}} \quad \forall g,k \tag{5a}$$

$$P(\tilde{\bar{P}}_{gen,g,k} \leq cap_g) \geq 1 - \epsilon_{\tilde{P}_{gen,g,k}} \quad \forall g,k \tag{5b}$$

Using Eq. (4a) to further specify $\tilde{\bar{P}}_{gen,g,k}$ in Eqs. (5a) and (5b), and reformulating the chance constraints into deterministic constraints following the same procedure as adopted by Bienstock et al. [46], the following expressions constraining the generator output, and constituting the set of feasible strategies X_g for a particular generator g, are obtained.

$$\bar{\tilde{P}}_{gen,g,k} \geq 0 + \Phi^{-1}(1-\epsilon_{\tilde{P}_{gen,g,k}})\,V_{g,k} \quad \forall g,k \tag{6a}$$

$$\bar{\tilde{P}}_{gen,g,k} \leq cap_g - \Phi^{-1}(1-\epsilon_{\tilde{P}_{gen,g,k}})\,V_{g,k} \quad \forall g,k \tag{6b}$$

$$V_{g,k} \geq \alpha_{g,k}\,\frac{1}{\Delta t}\left\|\begin{matrix} R_{1,k} \\ \vdots \\ R_{B,k} \\ \Delta t\,\sigma_{sys,k}\end{matrix}\right\|_2 \quad \forall g,k \tag{6c}$$

$$\alpha_{g,k} \geq 0 \quad \forall g,k \tag{6d}$$

Note that the elaboration of the 2-norm in Eq. (6c) results in the more comprehensible expression for the reserve capacity given by Eq. (7); the reformulation of this expression into the SOC constraint of Eq. (6c) is nevertheless required to guarantee the convexity of the optimization problem.

$$V^2_{g,k} \geq \alpha^2_{g,k}\,\frac{1}{\Delta t^2}\left(\sum_{b=1}^{B}\Sigma_{D_{b,k}} + \Sigma_{sys,k}\Delta t^2\right) \quad \forall g,k \tag{7}$$

Based on Eqs. (6a), (6b), (6c), and (6d), the scheduled supply of electric energy $\bar{S}_{g,k}$ and of reserve capacity $V_{g,k}$ can then be defined as follows:

$$\bar{S}_{g,k} = \bar{\tilde{P}}_{gen,g,k}\,\Delta t \quad \forall g,k \tag{8a}$$

$$V_{g,k} \quad \forall g,k \tag{8b}$$

2.1.3. Coupling constraints

The coupling constraints express the link between the demand side and the supply side. The first coupling constraint, Eq. (9), imposes the

[6] The coefficient of performance $\overline{COP}^{sh}_{b,k}$, which is temperature dependent, is estimated based on the weather forecast.

[7] For sake of simplicity, we opted not to include ramping constraints, or constraints on which types of assets can deliver reserve capacity [45,46]. Note that the inclusion of such constraints would render the supply side less flexible. This would increase the value of our approach, as it allows controlling the demand for real-time flexibility. As such, our results can be seen as a conservative estimate of the value of the flexibility available at the demand side.

required balance between supply of and demand for electric energy under expected conditions.

$$\sum_{g=1}^{G} \bar{S}_{g,k} = \sum_{b=1}^{B} \bar{D}_{b,k} + \bar{D}_{trad,k} \qquad \forall k \tag{9}$$

The second coupling constraint, Eq. (10), ensures that executing the affine control policy offsets the real-time deviations, i.e., $\sum_{g=1}^{G} \alpha_{g,k} = 1\ \forall k$, and that the provided reserve capacity matches the requested reserve capacity.

$$\sum_{g=1}^{G} V_{g,k} \geq \frac{1}{\Delta t} \left\| \begin{matrix} R_{1,k} \\ \vdots \\ R_{B,k} \\ \Delta t\, \sigma_{sys,k} \end{matrix} \right\|_2 \qquad \forall k \tag{10}$$

2.1.4. Objective function

As stated above, the integrated system-level optimization problem aims to minimize the overall system operating cost, determined by the day-ahead (and hence, expected) costs of energy, c_g^{EN}, reserve capacity provision, c_g^{REp}, and reserve capacity activation, c_g^{REa}.

The day-ahead energy and reserve capacity activation costs for a particular generator g are both determined by the expected cost of the stochastic generation, expressed by Eq. (11). The generation cost function c_g^{GEN} is assumed to be a quadratic function (characterized by three cost coefficients $c_{2,g}$, $c_{1,g}$ and $c_{0,g}$), in accordance with standard power system engineering practice [46,47].

$$\begin{aligned} \mathbb{E}[c_g^{GEN}(\tilde{S}_{g,k})] &= \mathbb{E}\left[\frac{c_{2,g}}{2}\tilde{S}_{g,k}^2 + c_{1,g}\tilde{S}_{g,k} + c_{0,g}\right] && \forall g,k \\ &= \frac{c_{2,g}}{2}\mathbb{E}[\tilde{S}_{g,k}^2] + c_{1,g}\mathbb{E}[\tilde{S}_{g,k}] + c_{0,g} && \forall g,k \end{aligned} \tag{11}$$

Taking into account the definition of the stochastic generation as introduced by Eq. (4a), the expected values $\mathbb{E}[\tilde{S}_{g,k}]$ and $\mathbb{E}[\tilde{S}_{g,k}^2]$ can be written as

$$\mathbb{E}[\tilde{S}_{g,k}] = \mathbb{E}\left[\bar{S}_{g,k} + \alpha_{g,k}\left(\sum_{b=1}^{B}\delta D_{b,k} + \delta w_{sys,k}\Delta t\right)\right] = \bar{S}_{g,k} \qquad \forall k \tag{12a}$$

and

$$\begin{aligned} \mathbb{E}[\tilde{S}_{g,k}^2] = \mathbb{E}\Bigg[&\bar{S}_{g,k}^2 + \alpha_{g,k}^2\left(\sum_{b=1}^{B}\delta D_{b,k}\right)^2 + \alpha_{g,k}^2\left(\delta w_{sys,k}\Delta t\right)^2 \\ &+ 2\,\alpha_{g,k}^2\left(\sum_{b=1}^{B}\delta D_{b,k}\right)\left(\delta w_{sys,k}\Delta t\right) \\ &+ 2\,\bar{S}_{g,k}\,\alpha_{g,k}\left(\sum_{b=1}^{B}\delta D_{b,k}\right) + 2\,\bar{S}_{g,k}\,\alpha_{g,k}\left(\delta w_{sys,k}\Delta t\right)\Bigg] && \forall g,k \\ = \bar{S}_{g,k}^2 + \alpha_{g,k}^2&\left(\sum_{b=1}^{B}\Sigma_{D_{b,k}} + \Sigma_{sys,k}\Delta t^2\right) && \forall g,k \end{aligned} \tag{12b}$$

taking advantage of the assumption that $\delta w_{sys,k}\ \forall k$ and $\delta D_{b,k}\ \forall b,k$ are all independent stochastic random variables, and all have zero mean.

Consequently, the expected cost of the stochastic generation can be expressed as follows.

$$\begin{aligned} \mathbb{E}\left[c_g^{GEN}(\tilde{S}_{g,k})\right] = &\frac{c_{2,g}}{2}\bar{S}_{g,k}^2 + c_{1,g}\bar{S}_{g,k} + c_{0,g} \\ &+ \frac{c_{2,g}}{2}\alpha_{g,k}^2\left(\sum_{b=1}^{B}\Sigma_{D_{b,k}} + \Sigma_{sys,k}\Delta t^2\right) \qquad \forall g,k \end{aligned} \tag{13}$$

By finally implementing Eq. (7) into Eq. (13), the following expressions for the day-ahead expected cost of energy c_g^{EN}, and the day-ahead expected cost of real-time reserve capacity activation c_g^{REa} for a particular generator g are obtained.

$$c_g^{EN} = \sum_{k=1}^{K}\frac{c_{2,g}}{2}\bar{S}_{g,k}^2 + c_{1,g}\bar{S}_{g,k} + c_{0,g} \quad \forall g \tag{14a}$$

$$c_g^{REa} \geq \sum_{k=1}^{K}\frac{c_{2,g}}{2}V_{g,k}^2\Delta t^2 \quad \forall g \tag{14b}$$

The cost of reserve capacity provision is assumed to be a percentage of the generation cost, here 30 %, as suggested by Pandžić et al. [48]. This leads to the expression given by Eq. (14c) for the day-ahead cost of reserve capacity provision c_g^{REp}. Note that this cost is based on the constraint tightening level $\Phi^{-1}(1-\epsilon_{\dot{P}_{gen,g,k}})V_{g,k}$ of the generator power constraints Eqs. (6a) and (6b), which reflects how much upward reserve capacity needs to be scheduled:

$$\begin{aligned} c_g^{REp} &= \sum_{k=1}^{K} 0.30\left(c_{2,g}\frac{cap_g}{2} + c_{1,g}\right)\left(\Phi^{-1}(1-\epsilon_{\dot{P}_{gen,g,k}})V_{g,k}\right) \\ &= \sum_{k=1}^{K} c_{3,g}\,\Phi^{-1}(1-\epsilon_{\dot{P}_{gen,g,k}})V_{g,k} \end{aligned} \tag{14c}$$

The summation of these three cost components for all involved electricity generation units characterizes the total system-level operating cost, and defines the objective function of the integrated system-level optimization problem.

$$\begin{aligned} &\sum_{g=1}^{G} c_g^{EN} + c_g^{REa} + c_g^{REp} \\ &\geq \sum_{g=1}^{G}\sum_{k=1}^{K}\frac{c_{2,g}}{2}\bar{S}_{g,k}^2 + c_{1,g}\bar{S}_{g,k} + c_{0,g} \\ &\quad + \sum_{g=1}^{G}\sum_{k=1}^{K}\frac{c_{2,g}}{2}V_{g,k}^2\Delta t^2 + \sum_{g=1}^{G}\sum_{k=1}^{K} c_{3,g}\,\Phi^{-1}(1-\epsilon_{\dot{P}_{gen,g,k}})V_{g,k} \end{aligned} \tag{15}$$

2.1.5. Resulting integrated system-level problem

The combination of the demand side constraints, supply side constraints, coupling constraints and objective function results in the following integrated system-level optimization problem (16).[8]

$$\min_{\substack{\{\chi_b\}_{b=1\ldots B} \\ \{\chi_g\}_{g=1\ldots G}}} \sum_{g=1}^{G} f_g(\bar{\mathbf{S}}_g, \mathbf{V}_g) \tag{16a}$$

with

$$\begin{aligned} f_g(\bar{\mathbf{S}}_g, \mathbf{V}_g) = \sum_{k=1}^{K}\Bigg(&\left(\frac{c_{2,g}}{2}\bar{S}_{g,k}^2 + c_{1,g}\bar{S}_{g,k} + c_{0,g}\right) + \left(\frac{c_{2,g}}{2}V_{g,k}^2\Delta t^2\right) \\ &+\left(c_{3,g}\,\Phi^{-1}(1-\epsilon_{\dot{P}_{gen,g,k}})V_{g,k}\right)\Bigg) \qquad \forall g \end{aligned} \tag{16b}$$

subject to

Demand side constraints:

$$\{\bar{\mathbf{D}}_b, \mathbf{R}_b, \mathbb{o}_b\} \in X_b, \text{ defined by Eqs. (3a)–(3p)} \qquad \forall b \tag{16c}$$

[8] The validity of the assumption of normality for each distinct state and input has been substantiated in our previous work [49,50], by investigating the kurtosis and skewness of the uncertain building model parameters, and of the forecast errors. Moreover, in Uytterhoeven et al. [21],Uytterhoeven [49] we showed that, despite this assumption, the considered SMPC^{ap} strategy is able to guarantee improved thermal comfort compared to the state-of-the-art in closed-loop simulations, where actual (non-Normally distributed) building model parameters and forecasts were used. The impact of the assumption of Gaussianity of all considered uncertainties, including the system-level uncertainty, could be more profoundly investigated by performing Monte Carlo simulations, to check whether the reformulated chance constraints (i.e., the thermal comfort requirements (Eqs. (2b) and (2c), the technical limits of the heating system (Eqs. (2e), (2f)) and the technical constraints regarding the output of the generators (eqs. (5a) and (5b)) are actually met by their respective probabilities of $1-\epsilon$. However, this would require a large number of closed-loop simulations, to be able to make profound, substantiated statements with sufficient confidence. Given the mathematical complexity of the stochastic optimal control problem, and the associated calculation effort, this is not further pursued in this paper. In this work, the focus is limited to the open-loop optimal control problem.

Table 1
Overview of the main characteristics of the nine renovated residential dwellings constituting the demand side of the integrated system-level optimization problem. For details, see p. 57 in Uytterhoeven [49].

Index	Building type [-]	Net floor area [m^2]	Protected volume [m^3]	Construction year [-]	UA-value floor, roof & walls [W/K]	UA-value windows [W/K]
1	Terraced	129	406	<1950	0.54	0.42
2	Terraced	193	531	<1950	0.57	0.43
3	Terraced	244	844	1950–1990	0.62	0.46
4	Semi-detached	155	546	1950–1990	0.37	0.38
5	Semi-detached	210	692	1950–1990	0.40	0.39
6	Semi-detached	275	742	<1950	0.31	0.36
7	Detached	163	559	1950–1990	0.36	0.35
8	Detached	260	716	<1950	0.31	0.35
9	Detached	301	752	>1990	0.34	0.36

Supply side constraints:

$$\{\bar{\mathbf{S}}_g, \mathbf{V}_g\} \in X_g, \text{ defined by Eqs. (6a)–(6d)} \qquad \forall g \qquad (16d)$$

Coupling constraints:

$$\sum_{g=1}^{G} \bar{S}_{g,k} = \sum_{b=1}^{B} \bar{D}_{b,k} + \bar{D}_{trad,k} \qquad \forall k \qquad (16e)$$

$$\sum_{g=1}^{G} V_{g,k} \geq \frac{1}{\Delta t} \left\| \begin{matrix} R_{1,k} \\ \vdots \\ R_{B,k} \\ \Delta t\, \sigma_{sys,k} \end{matrix} \right\|_2 \qquad \forall k \qquad (16f)$$

2.2. Distributed solution strategy using ADMM

The integrated system-level optimization problem is a fairly large problem, with a large number of optimization variables. To ensure mathematical tractability, we leverage a distributed solution approach for the integrated problem, splitting up the original problem into smaller subproblems (i.e., B subproblems for the different buildings and G subproblems for the different generators), each of which are easier to manage, and can be solved in parallel. A particular algorithm that is well suited for distributed convex optimization, due its good convergence properties and ease of implementation [51,52], and which has been gaining increasing popularity in a DR context [40,53–55], is ADMM.

Following these ADMM-based solution strategies for DR applications, the system-level optimization problem breaks down into a hierarchical structure, which can be interpreted as a day-ahead coordination framework between a master problem (i.e., the update of the dual variables/prices associated with the coupling constraints in response to changes in, e.g., demand and generation) and the individual subproblems for all participants (i.e., the update of the primal variables for all distinct generators and buildings, which individually optimize their operating schedule for the upcoming day based on the prices they receive). When primal and dual variables (i.e., price information) no longer change between iterations, the procedure has converged towards the optimal solution of the system-level problem. Note that the ADMM procedure can thus be viewed as a form of tâtonnement or price adjustment process, where the price is increased or decreased depending on whether there is an excess demand or supply, respectively, ultimately aiming to converge towards a balance between supply and demand [40,51,56]. The interpretation of ADMM as a coordination mechanism between different market players enables valuable research regarding market functioning. Moreover, since each market player is distinctly represented via its own subproblem, this coordination mechanism facilitates real-life implementation.

For the sake of brevity, we do not include the details of our implementation here. We refer the interested reader to Appendix 5. All optimization problems were coded using the JuMP package in Julia and solved using Gurobi.

3. Data & assumptions

The main aim of this paper is to illustrate the added value at system level of explicitly accounting for the closed-loop feedback aspect in the open-loop OCP of MPC strategies for TCLs participating in DR programs, when subject to uncertainties. We do this by comparing the overall system operating cost, obtained by solving the integrated system-level optimization problem discussed in Section 2.1, with and without ADF. Recall that enabling ADF allows making a trade-off between the demand for energy and for reserve capacity during the planning phase, thereby accommodating alterations of the control strategy in real time if needed, whereas omitting ADF means that all uncertainty related to the building and its heating demand needs to be managed at building level in the form of a more conservative, fixed control strategy. We consider an electric power system the size of and inspired by the (future) Belgian power system. In what follows, we discuss the parameterization of the demand side and supply side of our problem, together with other, more general assumptions.

3.1. Demand side

To compose the demand side, we consider nine residential buildings, for which the parametric uncertainty was characterized in our previous work [21,50]. The main characteristics of these buildings are summarized in Table 1. All buildings are renovated and equipped with a heat pump, which is sized according to the nominal heat demand with an additional safety factor of 1.5, to account for the additive as well as parametric uncertainties. For the installed heat emission system, both radiators and floor heating are considered.

All buildings are assumed to be subject to the same weather conditions, for which the measured weather data of 2016 of the Vliet test building of the KU Leuven Laboratory of Building Physics located in Leuven (Belgium), are used. The expected value and covariance of the weather forecasts, needed to characterize $\bar{\mathbf{d}}_{b,k}$ and $\Sigma^r_{\mathbf{d}_{b,k}}$, are determined by applying the methods described in Uytterhoeven et al. [21].

Regarding the occupant behavior, each of the nine buildings is combined with a different occupancy profile obtained from the open web tool StROBe (Stochastic Residential Occupancy Behavior) of Baetens et al. [57], which defines the internal heat gains and indoor temperature set-points (i.e. the lower thermal comfort bound).[9] The upper bound for the indoor air temperature T_{ia} (i.e., the state assumed to be directly linked to thermal comfort[10]), is determined as follows: $T^{\max}_{ia} = \max(\{T^{\min}_{ia,k}\}_{k=0\ldots K+1}) + \Delta T_{DR}$, where ΔT_{DR} defines the DR tem-

[9] StROBe generates random occupancy profiles, taking into account the number of occupants and the type of dwelling. The generated profiles are used consistently throughout all simulations (i.e., occupancy profiles are specific to each dwelling, but the same across all simulations).

[10] The thermal comfort is assessed based on the indoor air temperature, instead of on the operative temperature, which is used in comfort standards [42]. This

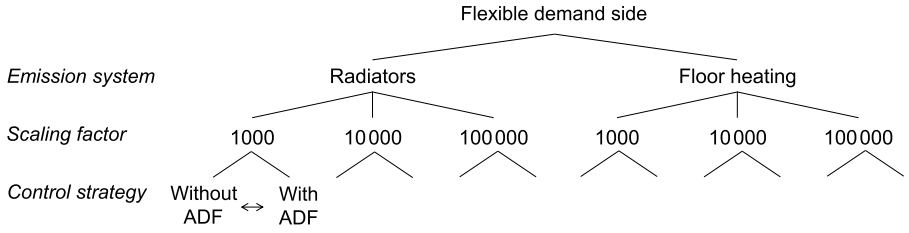

Fig. 1. The different scenarios for the flexible demand side as part of the integrated system-level problem.

perature band. In this work, ΔT_{DR} is set equal to 4°C (i.e., 2°C above and below the set-point) [35]. This wide DR temperature band ensures the existence of a feasible SMPC strategy with and without ADF. For a detailed discussion on this assumption, we refer the interested reader to Uytterhoeven [49] (p.182). Note that the maximum allowed temperature for DR is only based on the temperature set-points during the occupied period.

Each of the nine considered buildings is either controlled by an SMPC^{ap} strategy incorporating ADF, or by an equivalent strategy where ADF is disabled; both strategies consider a risk-averseness level regarding thermal comfort of $1-\boldsymbol{\epsilon}_{\mathbf{x}_{b,k}}=0.99$. The risk-averseness level associated with the input constraints, $1-\boldsymbol{\epsilon}_{\mathbf{u}_{b,k}}$, is taken equal to 0.999, to ensure compliance with the restrictive technical system limits to the best extent possible. The control strategies are determined for hourly time steps over a horizon of 60 hours to avoid end-of-horizon effects due to the large time constants of the buildings. However, only the first 24 hours are retained to compute the operating cost.

The demand determined by these control strategies is for each building scaled up by a constant factor. Three different scaling factors, representing different heat pump market penetration levels, are considered, being 1000, 10,000 or 100 000. This leads to a demand side population consisting of 9000, 90 000 or 900 000 flexible heat pumps, representing a market penetration level of approximately 0.2, 2 or 20 %.

As the heat pumps can either be coupled to radiators or floor heating, and can either be controlled by a strategy with or without ADF, a total number of 12 scenarios for the flexible demand side are considered, which are summarized in Fig. 1. The analysis is supplemented with one additional scenario, without any flexible heating demand, serving as a reference. Note that this final scenario can be calculated by centrally solving the integrated system-level optimization problem (16), with $\bar{\mathbf{D}}_b=\mathbf{R}_b=\mathbf{0}_K\ \forall b$; no distributed solution strategy is required in this case.

3.2. Supply side

Inspired by the Belgian power system, we consider a convex approximation of the merit order curve in the form of a piece-wise, linear function, with three segments representing three aggregated generators (GEN1, GEN2 and GEN3). The points demarcating the different segments of the piece-wise linear approximation of the merit order curve are (0,0), (5,40), (10,200) and (15,600), where the first value corresponds to the generation capacity (expressed in GW), and the second one to the marginal generation cost (expressed in EUR/MWh). As such, three aggregated generators (GEN1, GEN2 and GEN3) are discerned. The first two aggregated generators each represent a group of technologies with a total capacity of 5 GW; the capacity of the third, most expensive generator, on the other hand, is unbounded, to prevent feasibility issues. To prevent a generator to be scheduled to produce power beyond its capacity cap_g, small values are assigned to $\epsilon_{\dot{P}_{gen,g,k}}$ (here: 0.001), so that the chance constraints closely resemble the original hard constraints.

simplification is required because the radiative temperatures of the building components are not explicitly considered in the chosen building model.

Table 2
The cost coefficients describing the day-ahead cost of electric energy ($c_{2,g}, c_{1,g}$ and $c_{0,g}$) and reserve capacity provision ($c_{3,g}$) of the three aggregated generators constituting the supply side of the integrated system-level problem.

	GEN1	GEN2	GEN3
$c_{0,g}$ [EUR]	0	0	0
$c_{1,g}$ [EUR/MWh]	0	40	200
$c_{2,g}$ [EUR/MWh^2]	0.008	0.032	0.08
$c_{3,g}$ [EUR/MW]	6	36	120

Table 3
The four representative days for which the integrated system-level optimization problem is solved.

Day index	Date	Weighting factor
18	18th of January 2016	8.0
60	29th of February 2016	73.3
86	26th of March 2016	34.1
307	2nd of November 2016	95.6

The cost coefficients $c_{2,g}, c_{1,g}$ and $c_{0,g}$ describing the day-ahead expected cost of energy (see Eq. (14b)) for each of these aggregated generators are summarized in Table 2. Table 2 also shows the cost coefficients $c_{3,g}$ for the day-ahead cost of reserve capacity provision, which is assumed to be 30 % of the average marginal generation cost [48].

The fixed demand, supplementing the flexible demand of the heat pumps, is taken equal to the residual load profile of the Belgian power system, i.e., the total load profile reduced by the renewable supply. To ensure consistency, the used time series are also based on data for the year 2016, and are collected from the ENTSOE Transparancy Platform [58]. The time series of the renewable supply is rescaled in accordance with the currently installed renewable capacity.

Finally, the system-level uncertainty is assumed to be fixed, with $3\,\sigma_{sys}$ equal to 1 GW. This value reflects the largest contingency in the Belgian power system, being either the loss of a nuclear power plant, or the outage of the NEMO-link between Belgium and the UK serving as an important transmission asset [59].

3.3. Representative days

In order to limit the calculation time, the system-level operating cost is calculated for a set of representative days throughout the heating season (1st of October – 1st of April). With the method of Poncelet et al. [60], four representative days are identified, based on the time series for the ambient temperature, solar heat gains and residual loads throughout the heating season. The selected days are listed in Table 3. The weighing factors indicate how many days in the heating season are represented by a selected day. With the help of these weighting factors, results obtained for four days can be used to appraise the system behavior over the entire heating season. The associated weather conditions and non-flexible residual load profiles are depicted in Fig. 7 in the annex.

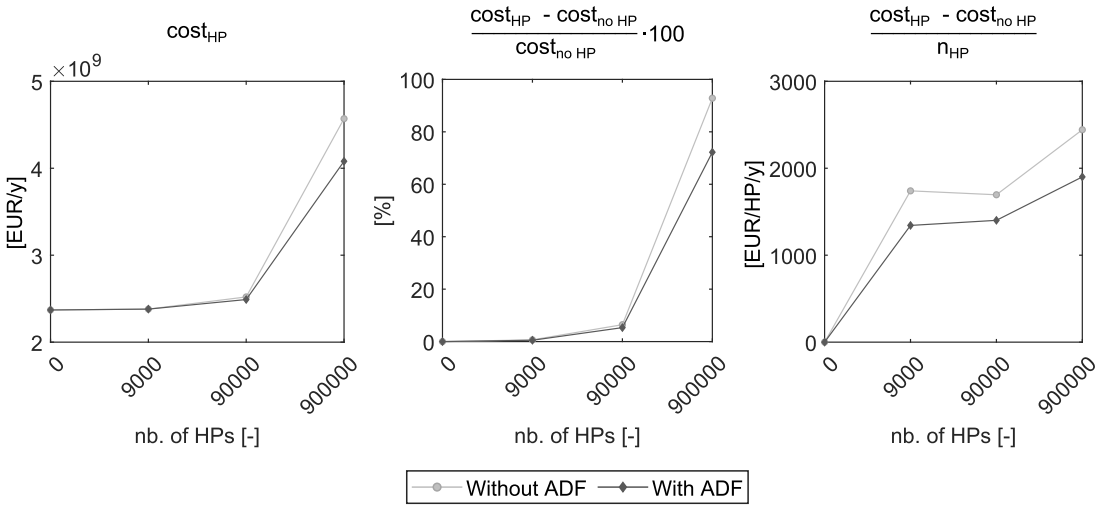

(a) In case of radiators.

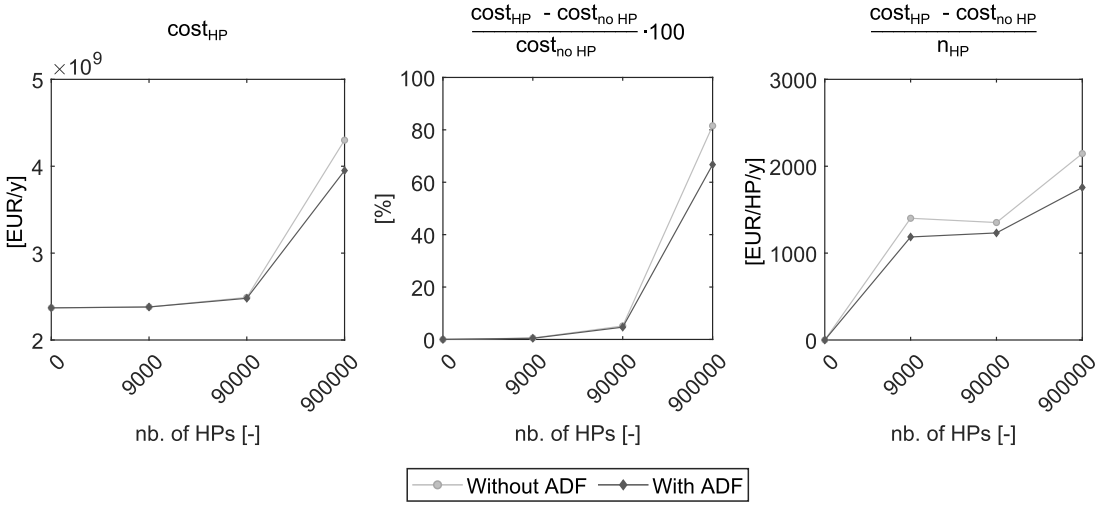

(b) In case of floor heating.

Fig. 2. The comparison of the total system operating cost over the entire heating season in case the demand side in the integrated system-level optimization problem is controlled by an SMPC^{ap} strategy with ADF, or by an equivalent strategy without ADF, for increasing heat pump market penetration levels and considering radiators (a) or floor heating (b). The figure shows the absolute operating cost (left), the relative cost increase compared to the reference case without flexible heat pumps (middle), and the absolute additional cost per heat pump compared to the reference case (right).

3.4. Solution strategy

In the ADMM procedure, the primal and dual stopping criteria, ϵ_{prim} and ϵ_{dual}, are set to 10^{-3}, as suggested by Boyd et al. [61]. The maximum number of iterations is set to 400, based on a series of trial-and-error simulations. The initial value for the penalty parameter ρ is set to 1, and is updated according to the adaptive scheme proposed by Boyd et al., in order to improve convergence, and to make the performance less dependent on the initially chosen value [61].

4. Results & discussion

Our results below show that the day-ahead coordination of the demand for reserve capacity, in addition to the demand for energy, enables a reduction of the system-level operating cost compared to the case where only the energy demand is coordinated. In the considered stylized case study, cost reductions up to 10.7 % are achieved, underpinning the added value of using MPC strategies incorporating ADF for DR under uncertainty.

In what follows, we first discuss the change in total operating cost (Section 4.1). Subsequently, we discuss the impact on the electricity generation and reserve capacity provision at the supply side (Section 4.2) and on the heating demand, the load uncertainty and the indoor temperature profile at the demand side (Section 4.3).

4.1. Impact on the energy system as a whole: total operating cost

Fig. 2 illustrates that the day-ahead coordination of the demand for reserve capacity, enabled by considering ADF, in addition to the demand for energy, induces a system operating cost reduction, which becomes more significant for increasing heat pump market penetration levels. This indicates that the implementation of the considered SMPC^{ap} strategy with ADF for DR under uncertainty contributes to a more cost-efficient electrification of the residential space heating sector. The analysis underpinning these results is performed for the case where all buildings are equipped with radiators (Fig. 2(a)), and the case where the buildings are equipped with underfloor heating (Fig. 2(b)). The system operating cost is shown in absolute numbers (left), as the relative cost

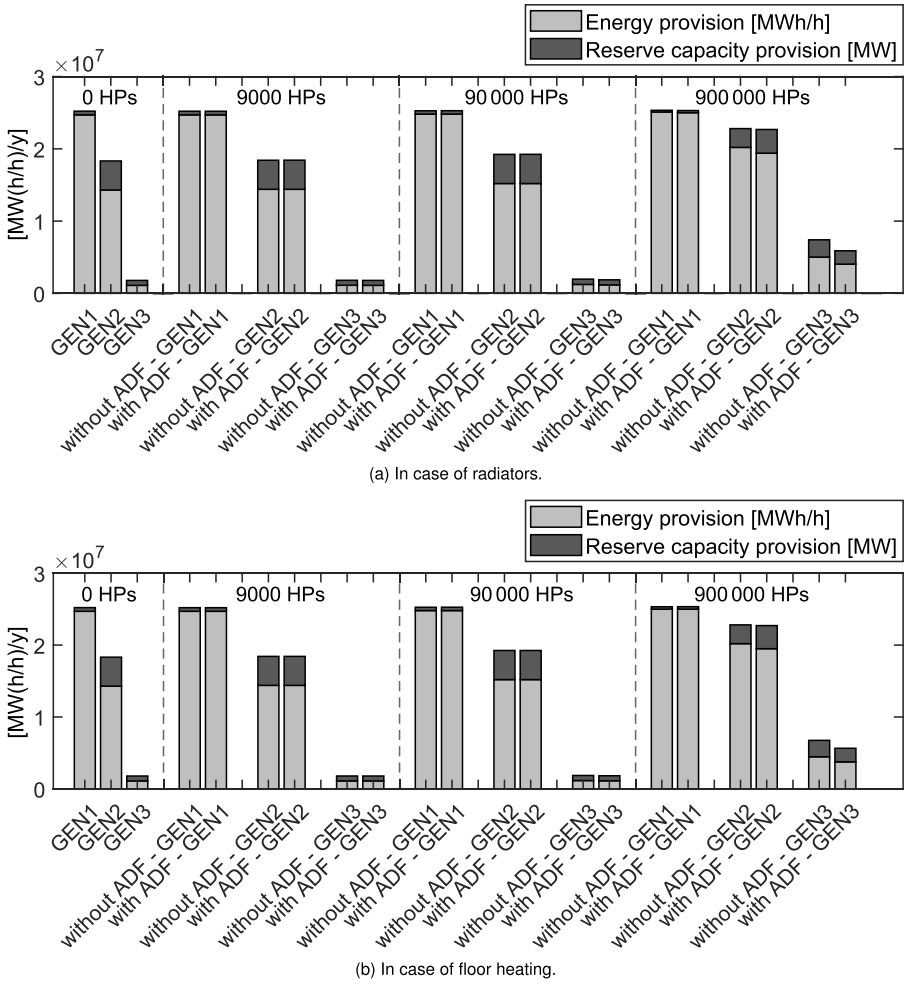

Fig. 3. Comparison of the optimized supply of electric energy and reserve capacity by the three aggregated generating facilities over the entire heating season in case the flexible demand side in the integrated system-level optimization problem is controlled by an SMPC^{ap} strategy with ADF, or by an equivalent strategy without ADF, for increasing heat pump market penetration levels, considering radiators (a) or floor heating (b).

increase compared to the reference case without heat pumps (middle) and as the additional cost per heat pump compared to the same reference case (right) for different market penetration levels of the flexible heat pumps.

A comparison of Fig. 2(a) and (b) demonstrates that the cost reductions induced by using the SMPC^{ap} strategy incorporating ADF are most pronounced for the case with radiators. In the case of a flexible demand side consisting of 9000, 90 000 or 900 000 heat pumps combined with radiators, the incorporation of ADF can induce an operating cost reduction of 0.2 %, 1.1 % or 10.7 % relative to the case without ADF. Considering floor heating, relative cost reductions of 0.1 %, 0.4 % and 8.1 % can be attained by incorporating ADF. In absolute terms, considering 9000, 90 000 or 900 000 heat pumps combined with radiators, the cost per heat pump per year is thanks to the incorporation of ADF reduced from 1747 EUR/HP/y to 1347 EUR/HP/y (reduction of 400 EUR/HP/y), from 1699 EUR/HP/y to 1404 EUR/HP/y (reduction of 295 EUR/HP/y), and from 2450 EUR/HP/y to 1907 EUR/HP/y (reduction of 543 EUR/HP/y). Considering floor heating, the cost per heat pump is reduced from 1407 EUR/HP/y to 1190 EUR/HP/y (reduction of 217 EUR/HP/y), from 1355 EUR/HP/y to 1235 EUR/HP/y (reduction of 120 EUR/HP/y), and 2151 EUR/HP/y to 1761 EUR/HP/y (reduction of 390 EUR/HP/y). The difference between the attainable gains with radiators or with floor heating is to be expected, since radiators are fast, responsive systems, which predominantly interact with the indoor air, meaning that their shift in operation is limited compared to the slower floor heating systems that interact through the building thermal mass, and hence have much larger time constants [62,63]. Consequently, an additional degree of freedom (i.e., the coordinated scheduling of the demand for reserve capacity, enabled through the ADF-based control strategy) for these faster systems with less thermal capacity has a higher impact on their flexibility.

4.2. *Impact on the supply side operation: Electricity generation and reserve capacity provision*

As illustrated in Fig. 3, the additional demand side flexibility made available by the SMPC^{ap} strategy with ADF shifts energy and reserve provision away from the third, most expensive generating unit (GEN3). For low market penetration levels (i.e., 9000 or 90 000 flexible heat pumps), the changes in operation of the different generators due to the additional coordination of the demand for reserve capacity are limited. Consequently, the marginal costs for the provision of energy and reserve capacity remain quasi unaltered, explaining the rather flat trends for the intermediate market penetration levels in the rightmost plots in Fig. 2. For the highest heat pump market penetration levels, the effect is more pronounced. Considering 900 000 heat pumps combined with radiators, the total energy supply by GEN3 over the entire heating season is reduced by 19.5 %, and the reserve capacity provision is reduced by 22.7 % relative to the case without ADF; the energy supply by GEN2, on the other hand, is reduced by 4.1 %, whereas the reserve capacity

provision is increased by 26.2 %. Considering floor heating, the energy supply by GEN3 is reduced by 15.8 %, and the reserve capacity provision is reduced by 16.9 % by incorporating ADF; the energy supply by GEN2 is reduced by 3.4 %, whereas the reserve capacity provision is increased by 23.0 %.

These different aspects regarding the altered supply side operation are also clearly visible in Fig. 4, showing the time-dependent stochastic generation profiles of the three aggregated generating facilities during the 29th of February, considering 900 000 heat pumps (arbitrarily chosen as an example). The shown uncertainty band surrounding the profile of the expected energy supply corresponds to the constraint tightening level of the generator power constraints, and thus reflects how much reserve capacity needs to be kept aside to cope with the uncertainty in the system.[11] For the cases with ADF, the generation output is clearly shifted downwards for GEN3. Moreover, expensive reserve capacity provided by GEN3 is replaced by cheaper reserve capacity provided by GEN2. This can be observed at t = 1417 h and t = 1427 h in Fig. 4. Finally, the peaks in required capacity are lower with ADF.

4.3. Impact on the demand side: Heating demand, load uncertainty and indoor temperature profile

The obtained operating cost savings and the altered supply side operation are enabled by the fundamentally different system behavior induced by incorporating ADF in the control strategy of the heat pumps, as illustrated in Fig. 5, showing the open-loop indoor temperature profiles and heat input profiles realized by an SMPC^{ap} strategy without or with ADF on the 29th of February for the detached, small, ageing (but renovated) dwelling (building 6 in Table 1) as part of the flexible demand side in the integrated system-level problem.

Without ADF, i.e., by prohibiting the closed-loop feedback aspect of MPC, all uncertainty needs to be managed at building level. Consequently, the uncertainty on the indoor air temperature is steadily growing as time proceeds, due to the accumulative effect of the additive and/or parametric uncertainties over the whole prediction horizon. This growing uncertainty results in an increasing constraint tightening level, which requires the mean indoor temperature $\bar{T}_{ia,k}$ to be progressively pushed further away from the lower bound, resulting in a rather high thermal energy demand, less flexibility to shift this energy demand to low-cost periods and, ultimately, higher system operating costs.

The incorporation of ADF allows for a less conservative control strategy, as the closed-loop feedback aspect of MPC in the open-loop control problem is considered. In other words, intermediate reactions against the additive and/or parametric uncertainties are enabled by ADF, which means that (i) the uncertainty on the system states can be reduced and (ii) managing the load uncertainty can be optimally coordinated between the building and system level. Since the required corrective actions depend on how severely the additive and/or parametric uncertainties manifest themselves in real time, the heat input now also becomes a stochastic variable (in contrast to the case without ADF).[12]

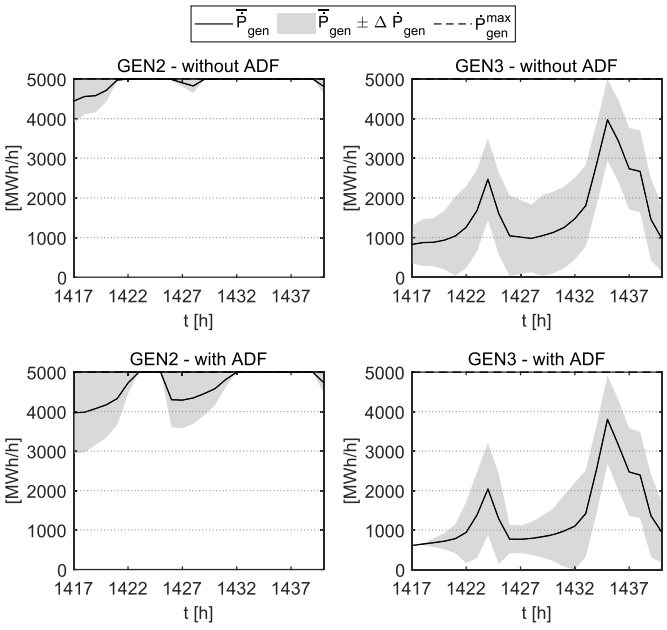

(a) In case of radiators.

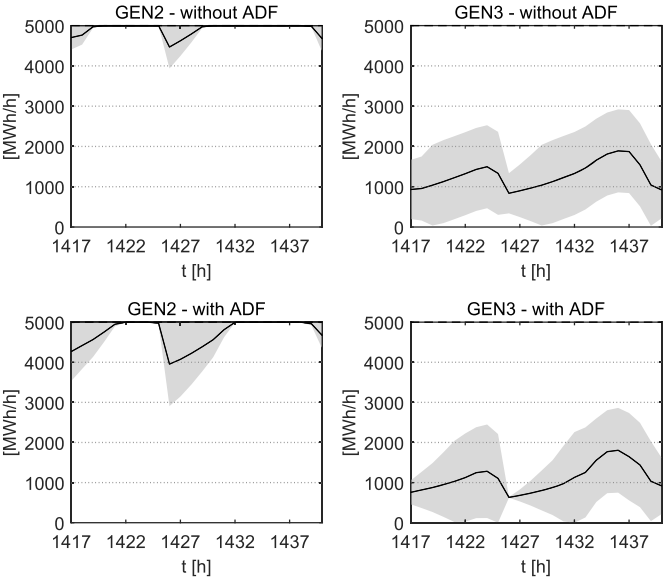

(b) In case of floor heating.

Fig. 4. Comparison of the open-loop stochastic generation profiles (averaged over one hour) of the three aggregated generating facilities during the 29th of February, in case the flexible demand side in the integrated system-level optimization problem, consisting of 900 000 flexible heat pumps, is controlled by the proposed SMPC^{ap} strategy, or by an equivalent strategy without ADF, in case of a demand side equipped with radiators (a) or with floor heating (b). Note GEN1 has been omitted, as its output is always equal to the maximum and it does not provide reserve capacity.

As a result,the energy demand is reduced, obviating the deployment of the more expensive generation units. In addition, the uncertainty on the temperature can be reduced in exchange for an increased uncertainty on the heat input, or in other words, the demand for energy can be partly traded for reserve capacity demand, allowing the more ex-

[11] To be precise, the uncertainty bands depicted in this paper delineate the intervals within which the actual values of the generator output, indoor temperature and heat input will fall with a probability of $1-2\epsilon_{\dot{P}_{gen,g,k}}$, $1-2\epsilon_{x_{i,k}}$ and $1-2\epsilon_{u_k}$. This particular choice for the uncertainty band is made for arguments of interpretability, as the constraint tightening level unequivocally reflects the operational freedom - either in the form of spare capacity or in the form of allowed temperature deviations - that needs to be provided to guarantee constraint satisfaction when subject to real-time perturbations in correspondence with the imposed risk-averseness level.

[12] The time profile established by the mean values $\{\bar{Q}_{sup,k}\}_{k=0\ldots K}$ should be viewed as the heat supply profile sustaining the optimized mean/reference indoor air temperature profile $\{\bar{T}_{ia,k}\}_{k=1\ldots K+1}$. The variance $\Sigma_{\bar{Q}_{sup,k}}$ at each time step k, on the other hand, characterizes the distribution of the possibly required real-time reaction against additive and/or parametric uncertainties that actually manifest themselves during $t = [0, k-1]$ in real time, in order to bring the perturbed temperature each time back to its reference profile at time step $k+1$.

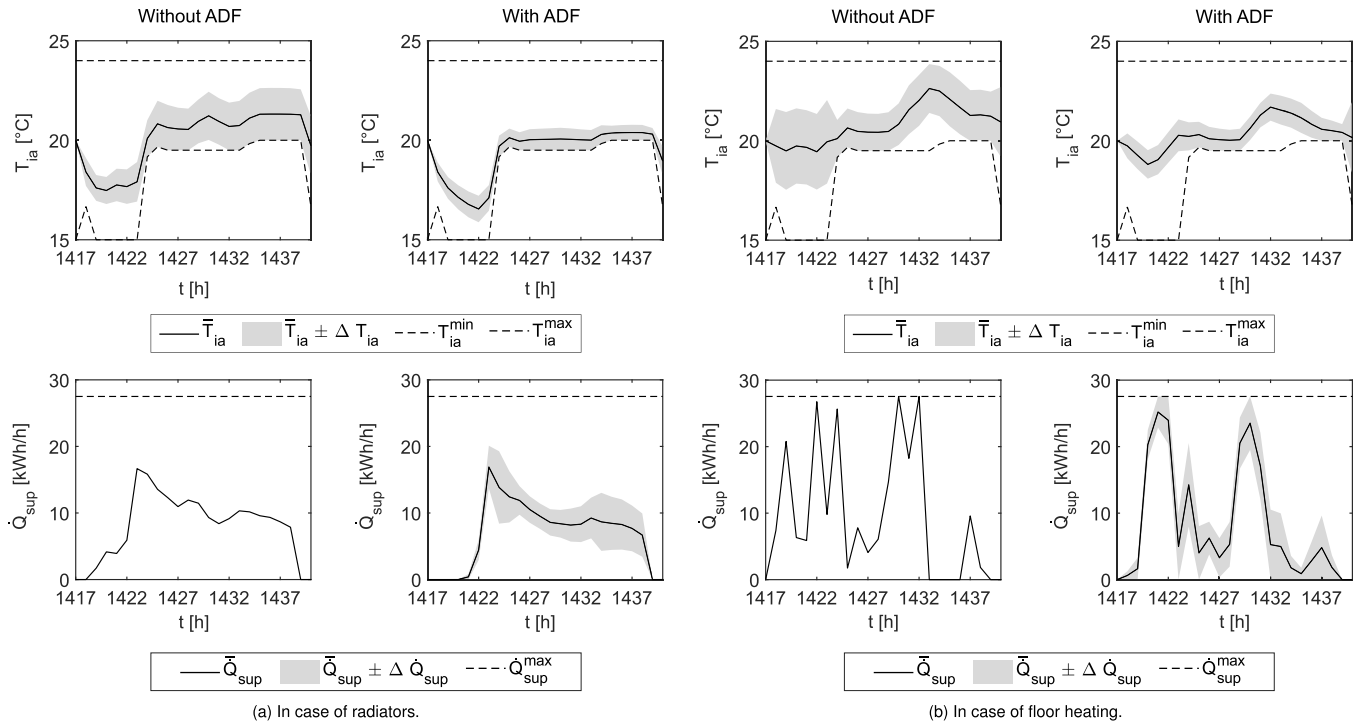

(a) In case of radiators. (b) In case of floor heating.

Fig. 5. The open-loop indoor temperature profiles and heat input profiles (averaged over one hour) realized by an SMPC^{ap} strategy without or with ADF during the 29th of February for the detached, small, ageing (but renovated) dwelling (building 6 in Table 1), either equipped with radiators (a) or with floor heating (b).

pensive supply of energy to be replaced by cheaper supply of reserve capacity.

Finally, Fig. 5 also clearly demonstrates the exploitation of the flexibility offered by the DR temperature band ΔT_{DR}. This is especially visible for the case with floor heating and the SMPC^{ap} strategy with ADF, where the stochastic temperature profile no longer necessarily sticks to the lower bound, such that a more desirable demand profile can be obtained to improve the system-level performance. Furthermore, it is important to note that the uncertainty band surrounding the mean temperature profile does not simultaneously hit the lower and upper temperature bounds at the end of the prediction horizon. This implies that there is still additional operational flexibility available. This remaining operational flexibility could not only be used to further adapt the profile of the demand for energy and reserve capacity, but can moreover also be exploited for reserve provision [64,66].

5. Conclusion and future research

This paper investigates the added value at system level of explicitly accounting for the closed-loop feedback aspect in the open-loop optimal control problem (OCP) of model predictive control (MPC) strategies for residential heat pumps (HPs) participating in demand response (DR) programs, when subject to uncertainties.

To this end, an integrated system-level optimization problem is set up, accounting for the mutual interaction between the supply and demand side, and aiming for a minimal system operating cost. The considered cost components include the day-ahead expected cost of electric energy, reserve capacity provision, and reserve capacity activation. The supply side constraints constituting the integrated problem are based on an economic dispatch problem. The demand side constraints, on the other hand, build upon a stochastic open-loop OCP formulation accounting for both additive and parametric uncertainties, derived in our previous work [21]. Here, two implementations are looked at, one with and one without affine disturbance feedback (ADF). ADF allows making a trade-off between the demand for energy and for reserve capacity during the planning phase, thereby accommodating alterations of the control strategy in real time if needed due to uncertainty manifestations; in other words, ADF unlocks an additional degree of freedom, which can be exploited in a DR context, to facilitate a more cost-effective use of the demand side flexibility offered by TCLs. The omission of ADF, on the other hand, means that all uncertainty related to the building and its heating demand needs to be managed at building level in the form of a more conservative, fixed control strategy; the latter approach can be considered as the current state-of-the-art for DR with MPC under uncertainty.

To ensure mathematical tractability, a distributed solution approach is proposed to solve the integrated system-level optimization problem, using the alternating direction method of multipliers (ADMM). By implementing this distributed optimization strategy, the integrated system-level optimization problem is converted into an hierarchical coordination framework that is communicating prices as a coordination signal to the different buildings and generators, to converge towards a balance between supply and demand.

The integrated system-level optimization problem is subsequently adopted in a case study, considering an electrification scenario of the residential heating sector. The flexible demand side, supplementing a fixed demand side characterized by a non-flexible demand and fixed system-level uncertainty, is constituted by a group of heterogeneous buildings equipped with compression heat pumps for space heating, each controlled by a stochastic MPC strategy, either with or without ADF. To maximize insight, different heat emission systems, and different market penetration levels are considered. The supply side, on the other hand, is constituted by three aggregated electricity generating facilities, whose techno-economical characteristics are inspired by the Belgian power system. To maintain tractability, the integrated system-level optimization problem is solved for a set of four representative days (18th of January 2016, 29th of February 2016, 26th of March 2016 and 2nd of November 2016), which can be used to appraise the system behavior over the entire heating season.

The results of this case study illustrate that the day-ahead coordination of the demand for reserve capacity, in addition to the demand for energy, enables a reduction of the system-level operating cost. The attainable gains in operating cost become more significant as the heat pump market penetration level increases, and are most prominent for a demand side where all buildings are equipped with radiators. In that case, with a heat pump market penetration level of approximately 20 %, i.e. 900 000 heat pumps, relative cost reductions up to 10.7 % are attainable, compared to 8.1 % in case of floor heating. In absolute terms, the cost per heat pump per year can be reduced from 2450 EUR/HP/y to 1907 EUR/HP/y for a demand side consisting of 900 000 flexible heat pumps coupled to radiators, and from 2151 EUR/HP/y to 1761 EUR/HP/y for an analogous demand side equipped with floor heating. Besides, it is shown that also a reduction in the required generation capacity might be achieved. These beneficial effects are shown to be caused by the fundamentally different demand side behavior induced by the incorporation of ADF in the stochastic MPC strategy, allowing for reduced conservatism, and for a possible interchange of the demand for electric energy and the demand for reserve capacity, compared to an equivalent strategy without ADF. This modified demand side behavior enables a more cost-efficient use of the available generating facilities and guarantees a more cost-efficient electrification of the residential space heating sector, thus showing the added value of incorporating ADF in robust/stochastic MPC strategies for DR under uncertainty.

The proposed hierarchical coordination framework can be interpreted as a solid basis for more dedicated research regarding system operation, market design, consumer coordination and tariff structures for DR under uncertainty. Indeed, additional modifications and extensions are required to correctly represent all underlying markets and associated market mechanisms, and the inclusion of all relevant market players (such as aggregators). Extending our optimization-based coordination framework to agent-based [33] or equilibrium models [34] would allow considering non-rational consumer behavior (e.g., limited attention to price signals or loss aversion) and distortions on the prices consumers receive (e.g., the imperfect coupling between wholesale and retail markets). Although this is not further pursued in this paper, it is recommended as a valuable track for future research. Future research could also focus on the interactions between different control strategies and sub-hourly dynamics in the supply and demand side.

Appendix ADMM

The integrated system-level optimization problem in the form of Problem (16) does not allow a decomposition of the problem into distinct subproblems for all different generators and buildings due to the considered formulation of the coupling constraints, Eqs. (16e) and (16f). This issue can be overcome by creating copies of the optimization variables involved in the coupling constraints, as for example done by Mhanna et al. [67] in the context of a quadratic second order cone constrained problem for optimal power flow. This duplication introduces additional auxiliary optimization variables ($\mathbf{z}_b^{EN}\ \forall b, \mathbf{z}_g^{EN}\ \forall g, \mathbf{z}_b^{RE}\ \forall b, \mathbf{z}_g^{RE}\ \forall g$), and new equality constraints linking the primal variables in the original coupling constraints to the auxiliary variables (not explicitly shown in the algorithm below), serving as renewed coupling constraints (with renewed associated dual variables). The problem can then be decomposed on these new equality constraints, whereas the original coupling constraints are relegated to the auxiliary problems. For the sake of brevity, we only discuss the resulting ADMM-based solution procedure below. For details on the required steps to cast the problem in a separable form and the derivation of the ADMM-based solution strategy, the interested reader is referred to Uytterhoeven [49].

The final algorithm to solve Problem (16) in an efficient, distributed way is schematically represented in Algorithm 1 and in Fig. 6, with l the iteration index. Throughout this iterative solution procedure, the dual variables ($\boldsymbol{\lambda}^{EN,l}, \boldsymbol{\lambda}_b^{RE,l}\ \forall b, \boldsymbol{\lambda}_g^{RE,l}\ \forall g$) serve as coordination signals for the generators and buildings, in order to ultimately align the supply and demand, while minimizing the overall system operating cost.

After initializing the dual and auxiliary variables, the first step (Step 1 in Algorithm 1) consists of solving the subproblems governing the optimization variables of all distinct buildings and generators. The objective of these subproblems consists of (i) the operating cost (only relevant for the generators), (ii) the cost of procuring or revenue of selling energy and reserve capacity and (iii) a quadratic penalty term, limiting the change in decision variables between iterations [61]. In the latter term, ρ is a hyper-parameter of the ADMM procedure [61].

The auxiliary variables update (Step 2 in Algorithm 1) breaks down into two separable subproblems for each time step, one per original coupling constraint (energy and reserve capacity, Eqs. (16e) and (16f)). For the auxiliary problem related to the energy balance constraint, a closed-form solution exists[13], resulting in two explicit expressions for the auxiliary variables $\mathbf{z}_g^{EN,l+1}\ \forall g$ and $\mathbf{z}_b^{EN,l+1}\ \forall b$. For the update of the auxiliary variables related to the reserve capacity balance constraint, on the other hand, we do not derive a closed-form solution. Although there exist closed-form solutions for projections onto second order cones (see e.g., Peng and Low [69]), the particular form considered in this paper is more complicated due to the presence of the constant $\Delta t\, \sigma_{sys,k}$ in the 2-norm in the constraint. Therefore, this auxiliary problem is retained (Step 2 - *Reserve capacity*), which is a well-manageable optimization problem with a low number of optimization variables.

[13] As discussed in Uytterhoeven [49], the subproblem to determine the auxiliary variables related to the energy balance constraint represents a Euclidean projection onto an affine set, which permits a clear-cut closed-form solution

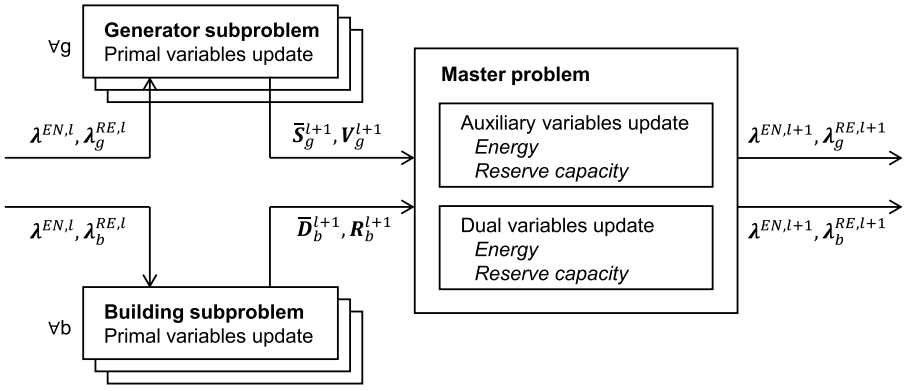

Fig. 6. Schematic representation of all different (primal/auxiliary/dual) update steps within one iteration of the distributed ADMM procedure, illustrating its hierarchical structure.

Algorithm 1 ADMM-based solution strategy for the integrated system-level optimization problem.

$\forall g, b : \boldsymbol{\lambda}^{EN,0}, \boldsymbol{\lambda}_b^{RE,0}, \boldsymbol{\lambda}_g^{RE,0}, \mathbf{z}_b^{EN,0}, \mathbf{z}_g^{EN,0}, \mathbf{z}_b^{RE,0}, \mathbf{z}_g^{RE,0} \leftarrow \mathbf{0}_K, \quad l \leftarrow 0$

while $\left\|\mathbf{res}_{prim}^{l+1}\right\|_2 > \epsilon_{prim}$ and $\left\|\mathbf{res}_{dual}^{l+1}\right\|_2 > \epsilon_{dual}$

Step 1: Primal variables update

Buildings

$$\forall b : \chi_b^{l+1} = \arg\min (\boldsymbol{\lambda}^{EN,l})^T \bar{\mathbf{D}}_b + (\boldsymbol{\lambda}_b^{RE,l})^T \mathbf{R}_b + \frac{\rho}{2} \left\| \begin{matrix} \bar{\mathbf{D}}_b - \mathbf{z}_b^{EN,l} \\ \mathbf{R}_b - \mathbf{z}_b^{RE,l} \end{matrix} \right\|_2^2$$

$$s.t. \quad \chi_b \in X_b, \text{ defined by Eqs. (3a)–(3p)}$$

Generators

$$\forall g : \chi_g^{l+1} = \arg\min \sum_{k=1}^{K} \left(\frac{c_{2,g}}{2} \bar{S}_{g,k}^2 + c_{1,g} \bar{S}_{g,k} + c_{0,g} + \frac{c_{2,g}}{2} V_{g,k}^2 \Delta t^2 + c_{3,g} \left(\Phi^{-1}(1 - \epsilon_{\hat{P}_{gen,g,k}}) V_{g,k} \right) \right)$$

$$- (\boldsymbol{\lambda}^{EN,l})^T \bar{\mathbf{S}}_g - (\boldsymbol{\lambda}_g^{RE,l})^T \mathbf{V}_g + \frac{\rho}{2} \left\| \begin{matrix} \mathbf{z}_g^{EN,l} - \bar{\mathbf{S}}_g \\ \mathbf{z}_g^{RE,l} - \mathbf{V}_g \end{matrix} \right\|_2^2$$

$$s.t. \quad \chi_g \in X_g, \text{ defined by (6a)–(6d)}$$

Step 2: Auxiliary variables update

Energy

$$\forall b : \mathbf{z}_b^{EN,l+1} = \bar{\mathbf{D}}_b^{l+1} + \frac{1}{G+B} \left(\sum_{g=1}^{G} \bar{\mathbf{S}}_g^{l+1} - \sum_{b=1}^{B} \bar{\mathbf{D}}_b^{l+1} - \bar{\mathbf{D}}_{trad} \right)$$

$$\forall g : \mathbf{z}_g^{EN,l+1} = \bar{\mathbf{S}}_g^{l+1} - \frac{1}{G+B} \left(\sum_{g=1}^{G} \bar{\mathbf{S}}_g^{l+1} - \sum_{b=1}^{B} \bar{\mathbf{D}}_b^{l+1} - \bar{\mathbf{D}}_{trad} \right)$$

Reserve capacity

$$\forall k : \left[\mathbf{z}_g^{RE,l+1}, \mathbf{z}_b^{RE,l+1} \right] = \arg\min_{\mathbf{z}} \sum_{g=1}^{G} \left\| z_{g,k}^{RE,l} - \left(V_{g,k}^{l+1} - \frac{\lambda_{g,k}^{RE,l}}{\rho} \right) \right\|_2^2 + \sum_{b=1}^{B} \left\| \left(R_{b,k}^{l+1} + \frac{\lambda_{b,k}^{RE,l}}{\rho} \right) - z_{b,k}^{RE} \right\|_2^2$$

$$s.t. \sum_{g=1}^{G} z_{g,k}^{RE} \geq \frac{1}{\Delta t} \left\| \begin{matrix} z_{1,k}^{RE} \\ \vdots \\ z_{B,k}^{RE} \\ \Delta t \ \sigma_{sys,k} \end{matrix} \right\|_2$$

Step 3: Dual variables update

Energy

$$\boldsymbol{\lambda}^{EN,l+1} = \boldsymbol{\lambda}^{EN,l} - \frac{\rho}{G+B} \left(\sum_{g=1}^{G} \bar{\mathbf{S}}_g^{l+1} - \sum_{b=1}^{B} \bar{\mathbf{D}}_b^{l+1} - \bar{\mathbf{D}}_{trad} \right)$$

Reserve capacity

$$\forall g : \boldsymbol{\lambda}_g^{RE,l+1} = \boldsymbol{\lambda}_g^{RE,l} + \rho \left(\mathbf{z}_g^{RE,l+1} - \mathbf{V}_g^{l+1} \right)$$

$$\forall b : \boldsymbol{\lambda}_b^{RE,l+1} = \boldsymbol{\lambda}_b^{RE,l} + \rho (\mathbf{R}_b^{l+1} - \mathbf{z}_b^{RE,l+1})$$

Step 4: Computing primal and dual residuals

$$\left\|\mathbf{res}_{prim}^{l+1}\right\|_2 = \left\| \begin{matrix} \mathbf{z}_g^{EN,l+1} - \bar{\mathbf{S}}_g^{l+1} \\ \bar{\mathbf{D}}_b^{l+1} - \mathbf{z}_b^{EN,l+1} \\ \mathbf{z}_g^{RE,l+1} - \mathbf{V}_g^{l+1} \\ \mathbf{R}_b^{l+1} - \mathbf{z}_b^{RE,l+1} \end{matrix} \right\|_2$$

$$\left\|\mathbf{res}_{dual}^{l+1}\right\|_2 = \left\| \begin{matrix} \rho \left(\mathbf{z}_g^{EN,l+1} - \mathbf{z}_g^{EN,l} \right) \\ \rho \left(\mathbf{z}_b^{EN,l+1} - \mathbf{z}_b^{EN,l} \right) \\ \rho \left(\mathbf{z}_g^{RE,l+1} - \mathbf{z}_g^{RE,l} \right) \\ \rho \left(\mathbf{z}_b^{RE,l+1} - \mathbf{z}_b^{RE,l} \right) \end{matrix} \right\|_2$$

$l \leftarrow l + 1$

end

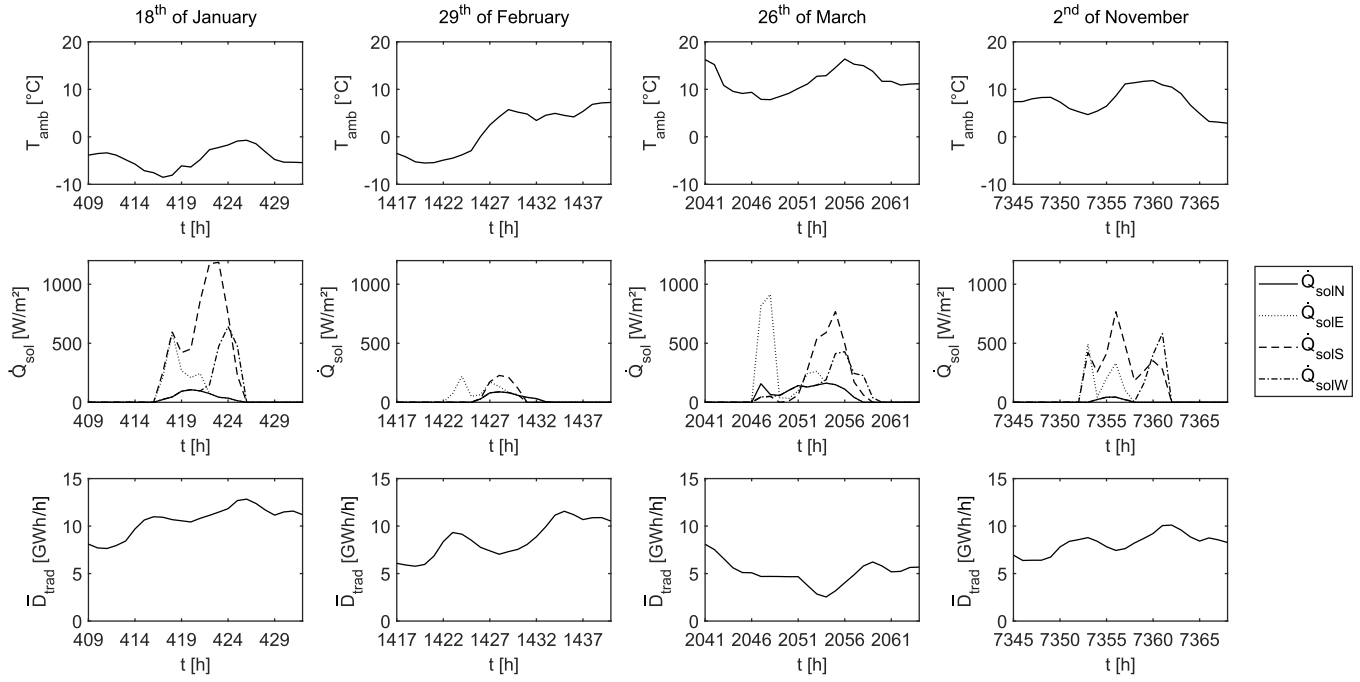

Fig. 7. The time profiles of the weather conditions (i.e., ambient temperature and solar heat gains) and of the non-flexible, residual load during the four representative days for which the integrated system-level optimization problem is being solved.

Step 3 in Algorithm 1 consists of updating the dual variables associated with the renewed coupling constraints (i.e., the new equality constraints creating copies, in the form of the auxiliary variables, of the optimization variables involved in the original coupling constraints). For the energy related coupling constraints, a single dual variable $\boldsymbol{\lambda}^{EN,l}$ suffices due to the existence of a closed-form solution to the auxiliary problem in Step 2. This dual variable is updated depending on the overall imbalance between the supply of and demand for electric energy. This unique dual variable $\boldsymbol{\lambda}^{EN,l}$ can be readily interpreted as the price for electric energy at which generators and buildings are exchanging commodities $\bar{\mathbf{S}}_g$ and $\bar{\mathbf{D}}_b$ [61]. Due to the specific problem structure, the dual variables associated with the reserve capacity related coupling (duplication) constraints $\{\boldsymbol{\lambda}_g^{RE,l}\ \forall g, \boldsymbol{\lambda}_b^{RE,l}\ \forall b\}$ cannot be reduced to a single dual variable. Rather, these dual variables are updated based on the imbalance between the projection of the supply of (demand for) reserve capacity onto the set defined by the original coupling constraints, $\mathbf{z}_g^{RE,l+1}$ ($\mathbf{z}_b^{RE,l+1}$), and the actual supply of (demand for) reserve capacity, $\mathbf{V}_g^{l+1}$ ($\mathbf{R}_b^{l+1}$) (which might not satisfy the original coupling constraints while searching for the optimal solution). Note that the balance between the projected supply and the projected demand is in turn enforced by solving the auxiliary problem related to the reserve capacity balancing constraint. Hence, the dual variables $\{\boldsymbol{\lambda}_g^{RE,l}\ \forall g, \boldsymbol{\lambda}_b^{RE,l}\ \forall b\}$ can still be interpreted as price signals, steered by the imbalance between supply and demand, albeit this time with an additional, intermediate step.

Last (Step 4 in Algorithm 1), the convergence of the iterative procedure towards the optimal solution is tracked with the help of the primal and dual residuals [51]. The primal residual, $\mathbf{res}_{prim}^{l+1}$, is a measure for the satisfaction of the coupling constraints, i.e., the imbalance between the auxiliary variables and the primal variables in the original coupling constraints. The dual residual, $\mathbf{res}_{dual}^{l+1}$, on the other hand, indicates how much the optimization variables still change from one iteration to the next. If these residuals are sufficiently small (i.e., smaller than the primal and dual stopping criteria, ϵ_{prim} and ϵ_{dual}), the iterative procedure is converged.

For more details, we refer the reader to Uytterhoeven [49].

Appendix Weather conditions in the four representative days

The weather conditions and non-flexible residual load profiles associated with the four representative days considered in the case study are visualized in Figure 7.

Data availability

Data will be made available on request.

Declaration of competing interest

No potential conflict of interest was reported by the authors.

CRediT authorship contribution statement

Anke Uytterhoeven: Writing – review & editing, Writing – original draft, Visualization, Validation, Software, Methodology, Investigation, Formal analysis, Data curation, Conceptualization; **Robbe Van Rompaey:** Writing – review & editing, Methodology, Conceptualization; **Lieve Helsen:** Writing – review & editing, Supervision, Project administration, Funding acquisition, Conceptualization; **Kenneth Bruninx:** Writing – review & editing, Supervision, Methodology, Conceptualization.

Acknowledgements

This work was supported by KU Leuven (C2 Research Project C24/16/018 'Energy Storage as a Disruptive Technology in the Energy System of the Future') and the Research Foundation – Flanders (FWO) (postdoctoral mandate 12J3320N). The computational resources and

[68]. Note this only holds if the energy balance constraint is formulated as an equality constraint.

services used in this work were provided by the VSC (Flemish Supercomputer Center), funded by the Research Foundation – Flanders (FWO) and the Flemish Government.

References

[1] European Commission, Communication from the Commission to the European Parliament, the Council, the European Economic and Social Committee and the Committee of the Regions. An EU strategy on heating and cooling, 2016, https://eur-lex.europa.eu/legal-content/EN/TXT/HTML/?uri=CELEX:52016DC0051. Accessed: 2021-05-17.

[2] European Commission, Directive 2018/844 of the European Parliament and of the Council of 30 May 2018 amending Directive 2010/31/EU on the energy performance of buildings and Directive 2012/27/EU on energy efficiency, 2018, https://eur-lex.europa.eu/legal-content/EN/TXT/HTML/?uri=CELEX:32018L0844. Accessed: 2021-05-17.

[3] European Commission, Directive (EU) 2018/2001 of the European Parliament and of the Council of 11 December 2018 on the promotion of the use of energy from renewable sources, 2018, https://eur-lex.europa.eu/legal-content/EN/TXT/HTML/?uri=CELEX:32018L2001. Accessed: 2021-05-17.

[4] G. Reynders, T. Nuytten, D. Saelens, Potential of structural thermal mass for demand-side management in dwellings, Building and Environment 64 (2013) 187–199.

[5] R.G. Junker, A.G. Azar, R.A. Lopes, K.B. Lindberg, G. Reynders, R. Relan, H. Madsen, Characterizing the energy flexibility of buildings and districts, Applied energy 225 (2018) 175–182.

[6] A. Arteconi, N.J. Hewitt, F. Polonara, State of the art of thermal storage for demand-side management, Applied Energy 93 (2012) 371–389. https://doi.org/10.1016/j.apenergy.2011.12.045

[7] G. Strbac, Demand side management: Benefits and challenges, Energy Policy 36 (12) (2008) 4419–4426. Foresight Sustainable Energy Management and the Built Environment Project, https://doi.org/10.1016/j.enpol.2008.09.030

[8] G. Bianchini, M. Casini, A. Vicino, D. Zarrilli, Demand-response in building heating systems: A Model Predictive Control approach, Applied Energy 168 (2016) 159–170.

[9] P. Siano, Demand response and smart grid-A survey, Renewable and Sustainable Energy Reviews 30 (2014) 461–478. https://doi.org/10.1016/j.rser.2013.10.022

[10] M. Avci, M. Erkoc, A. Rahmani, S. Asfour, Model predictive HVAC load control in buildings using real-time electricity pricing, Energy and Buildings 60 (2013) 199–209.

[11] R. Belmans, B. Beusen, B. Boesmans, W. Cardinaels, B. Claessens, S. Claessens, P. Coomans, R. Dhulst, W. De Meyer, J. Degraeve, C. Develder, B. Dupont, W. Foubert, J. Gordelbeke, F. Hoornaert, S. Iacovella, J. Jargstorf, R. Jahn, K. Kessels, W. Labeeuw, P. Muyters, S. Penninck, R. Ponnette, D. Six, S. Stoffels, J. Stragier, M. Strobbe, K. Van Daele, P. Van Dievel, P. Van Poppel, D. Vanbeveren, C. Vangrunderbeek, K. Vanthournout, G. Verbeek, P. Verboven, P. Vingerhoets, Linear: The Report. Demand Response for Families, Technical Report, 2014. https://www.energyville.be/sites/energyville/files/downloads/2020/boekje_linear_okt_2014_boekje_web.pdf. Accessed: 2021-08-17.

[12] D. Fischer, H. Madani, On heat pumps in smart grids: A review, Renewable and Sustainable Energy Reviews 70 (2017) 342–357. https://doi.org/10.1016/j.rser.2016.11.182

[13] F. Langner, W. Wang, M. Frahm, V. Hagenmeyer, Model predictive control of distributed energy resources in residential buildings considering forecast uncertainties, Energy and Buildings 303 (2024) 113753. https://doi.org/10.1016/j.enbuild.2023.113753

[14] P. Mohebi, S. Li, Z. Wang, Chance-constrained stochastic framework for building thermal control under forecast uncertainties, Energy and Buildings 331 (2025) 115385. https://doi.org/10.1016/j.enbuild.2025.115385

[15] M. Maasoumy, A. Sangiovanni-Vincentelli, Optimal control of building HVAC systems in the presence of imperfect predictions, in: 5th Dynamic Systems and Control Conference (DSCC) 2012 and 11th Motion and Vibration Conference (MOVIC) 2012, Fort Lauderdale, FL, USA, 45301, American Society of Mechanical Engineers (ASME) and Japan Society of Mechanical Engineers (JSME), 2012, pp. 257–266.

[16] F. Oldewurtel, A. Parisio, C.N. Jones, M. Morari, D. Gyalistras, M. Gwerder, V. Stauch, B. Lehmann, K. Wirth, Energy efficient building climate control using stochastic model predictive control and weather predictions, in: American Control Conference (ACC) 2010, Baltimore, MD, USA, IEEE, 2010, pp. 5100–5105.

[17] F. Oldewurtel, C.N. Jones, M. Morari, A tractable approximation of chance constrained stochastic MPC based on affine disturbance feedback, in: 47th IEEE Conference on Decision and Control (CDC) 2008, Cancun, Mexico, IEEE, 2008, pp. 4731–4736.

[18] F. Oldewurtel, A. Parisio, C.N. Jones, D. Gyalistras, M. Gwerder, V. Stauch, B. Lehmann, M. Morari, Use of model predictive control and weather forecasts for energy efficient building climate control, Energy and Buildings 45 (2012) 15–27.

[19] H. Nagpal, A. Staino, B. Basu, Robust model predictive control of HVAC systems with uncertainty in building parameters using linear matrix inequalities, Advances in Building Energy Research 14 (3) (2020) 338–354.

[20] F. Bunning, J. Warrington, P. Heer, R.S. Smith, J. Lygeros, Robust MPC with data-driven demand forecasting for frequency regulation with heat pumps, Control Engineering Practice 122 (2022) 105101. https://doi.org/10.1016/j.conengprac.2022.105101

[21] A. Uytterhoeven, R. Van Rompaey, K. Bruninx, L. Helsen, Chance constrained stochastic MPC for building climate control under combined parametric and additive uncertainty, J. Build. Perform. Simul. 15 (3) (2022) 410–430.

[22] C.A. Correa-Florez, A. Michiorri, G. Kariniotakis, Robust optimization for day-ahead market participation of smart-home aggregators, Applied energy 229 (2018) 433–445.

[23] C.A. Correa-Florez, A. Michiorri, G. Kariniotakis, Comparative analysis of adjustable robust optimization alternatives for the participation of aggregated residential prosumers in electricity markets, Energies 12 (6) (2019) 1019.

[24] G. Lankeshwara, R. Sharma, R. Yan, T.K. Saha, Control algorithms to mitigate the effect of uncertainties in residential demand management, Applied Energy 306 (2022) 117971.

[25] J. Hu, J. Cao, Demand Response Optimal Dispatch and Control of TCL and PEV Agents with Renewable Energies, Fractal and Fractional 5 (4) (2021) 140.

[26] H. Li, Z. Wan, H. He, Real-time residential demand response, IEEE Transactions on Smart Grid 11 (5) (2020) 4144–4154.

[27] J.L. Mathieu, M.G. Vayá, G. Andersson, Uncertainty in the flexibility of aggregations of demand response resources, in: 39th Annual Conference of the IEEE Industrial Electronics Society (IECON) 2013, Vienna, Austria, IEEE, 2013, pp. 8052–8057.

[28] M. Vrakopoulou, J.L. Mathieu, G. Andersson, Stochastic optimal power flow with uncertain reserves from demand response, in: 2014 47th Hawaii International Conference on System Sciences, IEEE, 2014, pp. 2353–2362.

[29] M. Vrakopoulou, B. Li, J.L. Mathieu, Chance constrained reserve scheduling using uncertain controllable loads Part I: Formulation and scenario-based analysis, IEEE Transactions on Smart Grid 10 (2) (2017) 1608–1617.

[30] Y. Zhang, S. Shen, J.L. Mathieu, Distributionally robust chance-constrained optimal power flow with uncertain renewables and uncertain reserves provided by loads, IEEE Transactions on Power Systems 32 (2) (2016) 1378–1388.

[31] N. Good, E. Karangelos, A. Navarro-Espinosa, P. Mancarella, Optimization under uncertainty of thermal storage-based flexible demand response with quantification of residential users' discomfort, IEEE Transactions on Smart Grid 6 (5) (2015) 2333–2342.

[32] X. Kou, F. Li, J. Dong, M. Olama, M. Starke, Y. Chen, H. Zandi, A Comprehensive Scheduling Framework using SP-ADMM for Residential Demand Response with Weather and Consumer Uncertainties, IEEE Transactions on Power Systems (2020).

[33] E. Sperber, C. Schimeczek, U. Frey, K.K. Cao, V. Bertsch, Aligning heat pump operation with market signals: aa win-win scenario for the electricity market and its actors?, Energy Rep. 13 (2025) 491–513. https://doi.org/10.1016/j.egyr.2024.12.028

[34] Y. Lu, C. Gorrasi, J. Meus, K. Bruninx, E. Delarue, System-wide benefits of temporal alignment of wholesale-retail electricity prices, Appl. Energy 373 (2024) 123857. https://doi.org/10.1016/j.apenergy.2024.123857

[35] D. Patteeuw, K. Bruninx, A. Arteconi, E. Delarue, W. D'haeseleer, L. Helsen, Integrated modeling of active demand response with electric heating systems coupled to thermal energy storage systems, Appl. Energy 151 (2015) 306–319. https://doi.org/10.1016/j.apenergy.2015.04.014

[36] N. O'Connell, P. Pinson, H. Madsen, M. O'Malley, Benefits and challenges of electrical demand response: a critical review, Renew. Sustain. Energy Rev. 39 (2014) 686–699.

[37] A. Nemirovski, A. Shapiro, Convex approximations of chance constrained programs, SIAM J. Optim. 17 (4) (2007) 969–996. https://doi.org/10.1137/050622328

[38] K. Garifi, K. Baker, B. Touri, D. Christensen, Stochastic Model Predictive Control for Demand Response in a Home Energy Management System, in: 2018 IEEE Power and Energy Society General Meeting (PESGM), IEEE, 2018, pp. 1–5.

[39] J. Wang, P. Li, K. Fang, Y. Zhou, Robust optimization for household load scheduling with uncertain parameters, Appl. Sci. 8 (4) (2018) 575.

[40] M. Diekerhof, F. Peterssen, A. Monti, Hierarchical distributed robust optimization for demand response services, IEEE Trans. Smart Grid 9 (6) (2017) 6018–6029.

[41] G. Lankeshwara, R. Sharma, Robust provision of demand response from thermostatically controllable loads using lagrangian relaxation, International Journal of Control 97 (8) (2024) 1918–1933. https://doi.org/10.1080/00207179.2023.2241579

[42] L. Peeters, R. De Dear, J. Hensen, W. D'haeseleer, Thermal comfort in residential buildings: comfort values and scales for building energy simulation, Appl. Energy 86 (5) (2009) 772–780.

[43] Y. Ma, J. Matuško, F. Borrelli, Stochastic model predictive control for building HVAC systems: complexity and conservatism, IEEE Trans. Control Syst. Technol. 23 (1) (2014) 101–116.

[44] A. Mirakhorli, B. Dong, Occupancy behavior based model predictive control for building indoor climate – A critical review, Energy Build 129 (2016) 499–513.

[45] K. Bruninx, Improved Modeling of Unit Commitment Decisions under Uncertainty, Ph.D. thesis, KU Leuven, Belgium, 2016.

[46] D. Bienstock, M. Chertkov, S. Harnett, Chance-constrained optimal power flow: risk-aware network control under uncertainty, SIAM Rev. 56 (3) (2014) 461–495.

[47] M. Zivic Djurovic, A. Milacic, M. Krsulja, A simplified model of quadratic cost function for thermal generators, in: 23rd International DAAAM Symposium 2012, Zadar, Croatia, 23, 2012, pp. 25–28.

[48] K. Pandžić, K. Bruninx, H. Pandžić, Managing risks faced by strategic battery storage in joint energy-reserve markets, IEEE Trans. Power Syst. 36 (5) (2021) 4355–4365.

[49] A. Uytterhoeven, Optimal Operation of Thermostatically Controlled Loads in Residential Buildings under Uncertainty: From a Building to an Electricity System Perspective, Ph.D. thesis, KU Leuven, Belgium, 2022. https://lirias.kuleuven.be/retrieve/653266[freelyavailable].

[50] A. Uytterhoeven, I. De Jaeger, K. Bruninx, D. Saelens, L. Helsen, Data-driven estimation of parametric uncertainty of reduced order RC models for building climate control, in: Building Simulation (BS) Conference 2021, Bruges, Belgium, International Building Performance Association (IBPSA), 2021.

[51] S. Boyd, N. Parikh, E. Chu, B. Peleato, J. Eckstein, Distributed Optimization and Statistical Learning via the Alternating Direction Method of Multipliers, 3, Now Publishers Inc, 2011.

[52] J. Eckstein, W. Yao, Augmented lagrangian and alternating direction methods for convex optimization: a tutorial and some illustrative computational results, RUTCOR Res. Rep. 32 (3) (2012) 44.
[53] J. Arroyo, S. Gowri, F. De Ridder, L. Helsen, Flexibility quantification in the context of flexible heat and power for buildings, in: REHVA Annual Meeting Conference Low Carbon Technologies in HVAC 2018, Brussels, Belgium, Federation of European Heating, Ventilation and Air Conditioning Associations (REHVA) and Royal Association of Heating, Ventilation and Climate Control Technology (ATIC), 2018.
[54] X. Kou, F. Li, J. Dong, M. Starke, J. Munk, Y. Xue, M. Olama, H. Zandi, A scalable and distributed algorithm for managing residential demand response programs using alternating direction method of multipliers (ADMM), IEEE Trans. Smart Grid 11 (6) (2020) 4871–4882.
[55] A. Mercurio, A. Di Giorgio, F. Purificato, Optimal fully electric vehicle load balancing with an ADMM algorithm in smart grids, in: 21st Mediterranean Conference on Control and Automation (MED) 2013, Crete, Greece, IEEE, 2013, pp. 119–124.
[56] H. Höschle, Capacity Mechanisms in Future Electricity Markets, Ph.D. thesis, KU Leuven, Belgium, 2018.
[57] R. Baetens, D. Saelens, Modelling uncertainty in district energy simulations by stochastic residential occupant behaviour, J. Build. Perform. Simul. 9 (4) (2016) 431–447. https://doi.org/10.1080/19401493.2015.1070203
[58] The European Network of Transmission System Operators for Electricity (ENTSO-E), ENTSO-E Transparancy Platform, (2021). https://transparency.entsoe.eu/. Accessed: 2021-09-13.
[59] Elia, Adequacy and flexibility study for Belgium 2020–2030, Technical Report, 2019.
[60] K. Poncelet, H. Höschle, E. Delarue, A. Virag, W. D'haeseleer, Selecting representative days for capturing the implications of integrating intermittent renewables in generation expansion planning problems, IEEE Trans. Power Syst. 32 (3) (2016) 1936–1948.
[61] S. Boyd, S.P. Boyd, L. Vandenberghe, Convex Optimization, Cambridge University Press, 2004.
[62] Z. Wang, B. Lin, Y. Zhu, Modeling and measurement study on an intermittent heating system of a residence in Cambridgeshire, Build. Environ. 92 (2015) 380–386.
[63] G. Reynders, Quantifying the Impact of Building Design on the Potential of Structural Storage for Active Demand Response in Residential Buildings, Ph.D. thesis, KU Leuven, Belgium, 2015.
[64] K. Bruninx, Y. Dvorkin, E. Delarue, W. D'haeseleer, D.S. Kirschen, Valuing demand response controllability via chance constrained programming, IEEE Trans. Sustain. Energy 9 (1) (2017) 178–187.
[65] K. Bruninx, H. Pandžić, H. Le Cadre, E. Delarue, On the interaction between aggregators, electricity markets and residential demand response providers, IEEE Transactions on Power Systems 35 (2) (2019) 840–853.
[66] G. De Zotti, S.A. Pourmousavi, H. Madsen, N.K. Poulsen, Ancillary services 4.0: a top-to-bottom control-based approach for solving ancillary services problems in smart grids, IEEE Access 6 (2018) 11694–11706.
[67] S. Mhanna, G. Verbič, A.C. Chapman, Accelerated methods for the SOCP-relaxed component-based distributed optimal power flow, in: Power Systems Computation Conference (PSCC) 2018, Dublin, Ireland, IEEE Power and Energy Society (PES), 2018, pp. 1–7. https://doi.org/10.23919/PSCC.2018.8442892
[68] J. Plesník, Finding the orthogonal projection of a point onto an affine subspace, Linear Algeb. Appl. 422 (2–3) (2007) 455–470.
[69] Q. Peng, S.H. Low, Distributed optimal power flow algorithm for radial networks, i: balanced single phase case, IEEE Trans. Smart Grid 9 (1) (2016) 111–121.